Table of Contents

Tables List

Figures List

List of Symbols

A_{cost} = price conversion of hydrogen ($/mol → $/kg)

A_{aero} = the contact area of the windshield and the air

a_{acc} = the accleration of vehicle

$a_{red/ox}$ = chemical activity of oxidized and reduced (activity

= concentration

× activity coefficient, where [ox]is oxidized, [red]is reduced)

C_{rr} = the coefficient of friction

C_x = the drag coefficient

C_{Ch} = charging cycles during the operating process

E_{cell} = cell voltage (V)

$E_{r,T,P}$ = reversible voltage according to temperature and pressure (V)

F = the faraday constant (96,485.3365 C/mol)

F_{acc} = the power of acceleration

F_r = the friction power of tire

F_{ad} = the resistance of aerodynamic drag

F_{cr} = the resistance of climbing

g = the gravity ($9.8N/kg$)

I_{Re} = the recharging current (A)

I_{ch} = charging current (A)

i_{cell} = the current density of the cell (A/cm^2)

i_L = the loss of current (A/cm^2)

i_0 = the exchange current reference (A/cm^2)

j_{lim} = the current density limit(A/cm^2)

L_B = life of battery

L'_B = improved battery life which is optimized by DOD controlling

$\boldsymbol{m_{total}} = \ the\ mass\ of\ vehicle\ and\ fuel\ cell$

$\boldsymbol{N_{fc}} = \ the\ number\ of\ fuel\ cell\ series$

$\boldsymbol{n_{electron}} = \ the\ number\ of\ electrons\ involved\ in\ the\ reaction(mol)$

$\boldsymbol{n_{half}} = \ the\ number\ of\ half-electron\ transfer\ reaction\ (mol)$

$\boldsymbol{n_B} = number\ of\ batteries$

$\boldsymbol{n_f} = the\ number\ of\ fuel\ cell\ series$

$\boldsymbol{P_B} = single\ battery\ price$

$\boldsymbol{P_{fuel}} = \ the\ price\ of\ fuel\ (hydrogen)$

$\boldsymbol{R_i} = \ the\ internal\ resistance\ (\Omega/cm^2)$

$\boldsymbol{R_{gas}} = \ the\ ideal\ gas\ constant\ (8.314472\ J \times K^{-1} \times mol^{-1})$

$\boldsymbol{t'} = modified\ charging\ time\ which\ is\ shortened\ by\ pulse\ charging\ method$

$\boldsymbol{T} = \ the\ temperature\ (K)$

$\boldsymbol{\alpha_{slop}} = \ the\ slop\ of\ ground$

$\boldsymbol{\alpha_{transfer}} = \ the\ transfer\ coefficient\ (n/a)$

$\boldsymbol{\rho_{air}} = \ the\ density\ of\ air$

$\boldsymbol{\lambda} = \ empirical\ factor\ of\ the\ water\ content\ in\ \ proton\ exchange\ membrane$

$\boldsymbol{\eta} = Faraday\ efficiency\ of\ fuel\ cell$

$[\boldsymbol{oxidized}]/[\boldsymbol{reduced}]$ *It represents the concentration of all the substances involved in the electrode reaction ratio of the concentration of the product and the product of the reaction products. And the concentration should be equal to the square of their second coefficient in the electrode reaction*

Rapport-Gratuit.com

Chapter 1 - Introduction

The purpose of this chapter is to describe the background and status of the new energy industry. The classification and the characterization of the fuel cell and electric vehicles will be introduced in this chapter. Additionally, the study will be launched around the hybrid electric truck – Nemo.

1.1 Fuel cell

Fuel cell is a generator which produces electricity by the chemical energy. Hydrogen is mostly used as the fuel, sometime, hydrocarbons such as natural gas and alcohols like methanol are also used[1].

In 1838, the first fuel cells were invented. A century later, NASA uses the fuel cell to supply the power for probes, satellites and space capsules[2]. From then on, the fuel cell became widely use in many area, such as: forklifts, automobiles, buses, airplanes, boats, motorcycles and submarines[1][3].

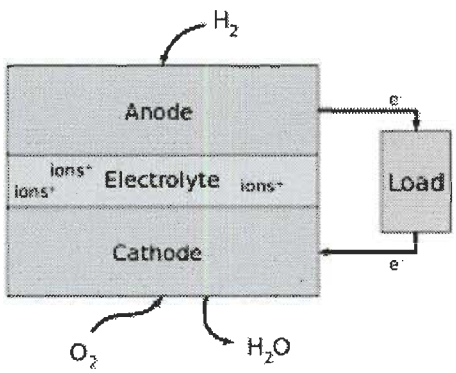

Figure 1-1. Fuel cell block diagram[4]

Fuel cells have many varieties, such as alkaline fuel cell, phosphoric acid fuel cell, molten carbonate fuel cell, etc. They are made up of three adjacent segments: the anode,

the electrolyte and the cathode. Two chemical reactions occur at the interfaces of the three different segments. The net result of the two reactions is that fuel is consumed and at the same time water and carbon dioxide is produced as byproducts. The main production is electric current[5].

1.1.1 Classification and characteristics

Fuel cell can be classified in many species and they are designed separately by their required working environment. According to their operating temperature, efficiency, volume and power, they can be equipped on different devices or buildings. In the researching and developing of electric vehicles, an important classification rule is the operating temperature[1].

Some popular species of fuel cells are introduced in the following table:

Table 1-1. Operation parameters of some common used fuel cells[6]

Fuel cell name	Electrolyte	Qualified power	Operating temperature (°C)	Efficiency (cell)	Efficiency (system)
Alkaline fuel cell (AFC)	Aqueous alkaline solution	10 – 100 kW	< 80	60–70%	62%
Proton exchange membrane fuel cell (PEMFC)	Polymer membrane	100 – 500 kW	50–100	50–70%	30–50%
Phosphoric acid fuel cell (PAFC)	Molten phosphoric acid (H_3PO_4)	< 10 MW	150-200	55%	40%
Molten carbonate fuel cell (MCFC)	Molten alkaline carbonate	100 MW	600–650	55%	47%
Planar Solid oxide fuel cell (SOFC)	O^{2-}-conducting ceramic oxide	<100 MW	500–1100	60–65%	55–60%

Compared with the other types of fuel cell (Table 1-1), PEMFC is the best candidate to be installed in the electric vehicles because of its low operating temperature. Although the

Rapport-gratuit.com
LE NUMERO 1 MONDIAL DU MÉMOIRES

system efficiency and the output power of PEMFC are not the highest, the low operating temperature is the most important element in the automotive area. It doesn't need to be outfitted additional insulation and heat dissipation devices.

1.1.1.1 AFC

Alkaline fuel cell (AFC) technology is the first proven fuel cell technology which is applied in NASA's space program[7].

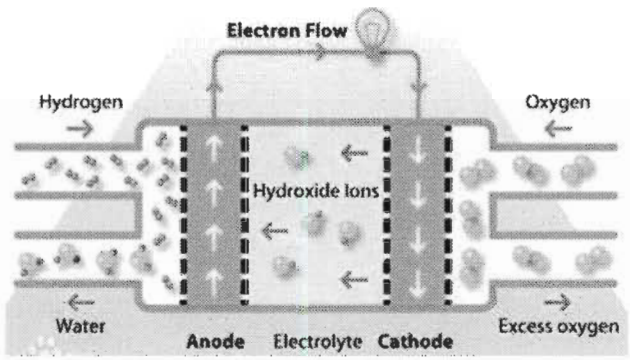

Figure 1-2. Structure of alkaline fuel cells[8]

The electrolyte used in the AFC is the aqueous solution or a stable potassium hydroxide matrix. In most types of fuel cell, hydroxyl moves from the cathode to the anode and reacts with hydrogen to generate water and ions. However, the reaction of AFC is different. These electrons are used to provide energy to an external circuit. Then, these electrons return to the cathode and react with oxygen to generate more hydroxyl ions.

Anode reaction:

$$O_2 + 2H_2O + 4e^- \rightarrow 4OH^-$$

Cathode reaction:

$$2H_2 + 4OH^- \rightarrow 4H_2O + 4e^-$$

The operating temperature of the alkaline fuel cell is about 80°C. Therefore, the start time comes short. However, its electricity density is ten times lower than the proton exchange membrane fuel cell. Additionally, being installed in vehicles makes the AFC appear to be clumsy. But their production cost is the lowest among all the fuel cells. That is why they

can be used as the small stationary power generation apparatus.

Alkaline fuel cells are very sensitive to carbon monoxide and other impurities will pollute the catalysts[9]. In addition, the electrolyte should not contain carbon because the carbon dioxide can react with potassium hydroxide and form potassium carbonate. Under these situations, the fuel cell's performance will be lowered.

1.1.1.2 SOFC

A solid oxide fuel cell (SOFC) is an electrochemical conversion device which produces electricity directly from oxidizing fuel. Solid oxide fuel cell (Solid Oxide Fuel Cell, referred SOFC) is the third generation fuel cell. The chemical will be stored in a direct fuel and oxidizer at high temperature. It is generally considered to be widely applied in the future.

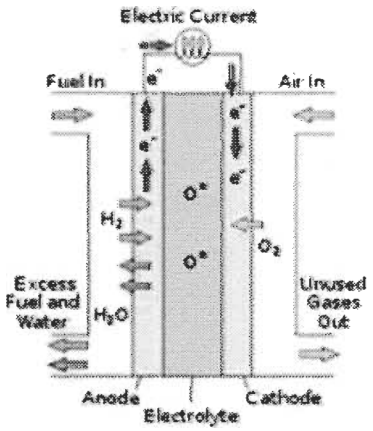

Figure 1-3. Operating principle of solid oxide fuel cell[2]

In all fuel cells, SOFC operating temperature is the highest. It belongs to the type of high temperature fuel cells. In recent years, distributed power station became an important part of the world's energy supply due to its low cost, high maintainability and some other advantages. Since SOFC power generation has high exhaust temperatures, has high value in use, can provide natural gas reforming heat required can also be used to produce steam. Additionally, the composition cycle of the gas turbine is the ideal mode of distributed generation. Fuel cells， gas turbines, steam turbines and other co-generation system not

only have high power generation efficiency, but also have low-pollution environmental benefits.

1.1.1.3 PAFC

Presently, phosphoric acid fuel cell (PAFC) is a fuel cell which grows fastest in commercialization. Phosphoric acid solution is used as the electrolyte in PAFC which is usually placed in the silicon carbide substrates. The operating temperature of phosphoric acid fuel cell is slightly higher than the proton exchange membrane fuel cells. However, the expensive platinum electrode catalyst inside which is used to accelerate the reaction is still irreplaceable[10].

Anode reaction:

$$2H_2 \rightarrow 4H^+ + 4e^-$$

Cathode reaction:

$$O_2 + 4H^+ + 4e^- \rightarrow 2H_2O$$

Overall cell reaction:

$$2H_2 + O_2 \rightarrow 2H_2O$$

The efficiency of phosphoric acid fuel cell is lower than other fuel cells (about 40%). Simultaneously, the heating time is longer than others.

1.1.1.4 MCFC

Molten carbonate fuel cell (MCFC) is a high temperature fuel cell (about 650°C). It uses a molten carbonate salt suspended in a porous ceramic matrix as the electrolyte. Salts commonly used include lithium carbonate, potassium carbonate and sodium carbonate[11].

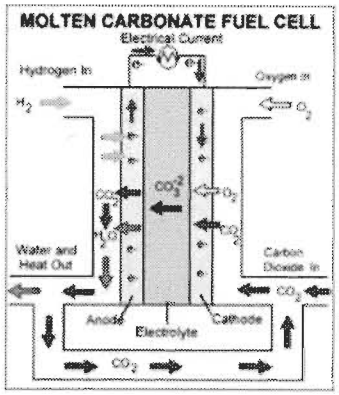

Figure 1-4. Operating principle of molten carbonate fuel cell[2]

The reaction principle is as follows:

Anode:

$$O_2 + 2CO_2 + 4e^- \rightarrow 2CO_3^{2-}$$

Cathode:

$$2H_2 + 2CO_3^{2-} - 4e^- \rightarrow 2CO_2 + 2H_2O$$

Total:

$$O_2 + 2H_2 \rightarrow 2H_2O$$

It has features such as high efficiency (greater than 40%), low noise, no pollution, fuel diversification (hydrogen gas, natural gas and bio-fuels etc.), waste heat utilization of high-value and low-cost battery construction materials and many other advantages. It hopes to be the green energy storage in the next century[12].

Molten carbonate fuel cells (MCFC) can also use NiO as the porous cathode. However, since the NiO which dissolved in molten carbonate can be reduced to Ni by H_2 and CO. This easily provokes a short circuit.

1.1.2 PEMFC

Proton exchange membrane fuel cell (PEMFC) uses a water-based and acidic polymer membrane as its electrolyte. The platinum-based is used as the electrodes[13]. The single unit cell is composed of an anode, a cathode and a proton exchange membrane. Hydrogen in anode reacts with the oxygen in cathode through the proton exchange membrane.

Additionally, the catalyst on the electrode will accelerate this slow reaction[14].

1.1.2.1 Principle of PEMFC

Anode reaction:

$$2H_2 \rightarrow 4H^+ + 4e^-$$

Cathode reaction:

$$O_2 + 4e^- + 4H^+ \rightarrow 2H_2O$$

Overall reaction:

$$H_2 + \frac{1}{2}O_2 \rightarrow H_2O$$

Since the proton exchange membrane only conducts protons. Therefore, the proton exchange membrane can directly reach the cathode and the electrons can only go to the cathode through the external circuit. When electrons flow to the cathode through the external circuit, current is generated. Superimposing several fuel cells can build up the fuel cell stack in order to match the different output voltage requirements in the practical application.

1.1.2.2 Structure

In the central of the PEM fuel cell, the membrane electrode assembly (MEA) is set (Figure 1-5). It is typically sandwiched by two flow field plates that are often mirrored. This structure can make a bipolar plate that is easily to be series connected when the cells should be stacked for greater voltages. The MEA consists of a proton exchange membrane, catalyst layers, and gas diffusion layers (GDL). These components are fabricated separately and then pressed to together at high temperatures and pressures[15].

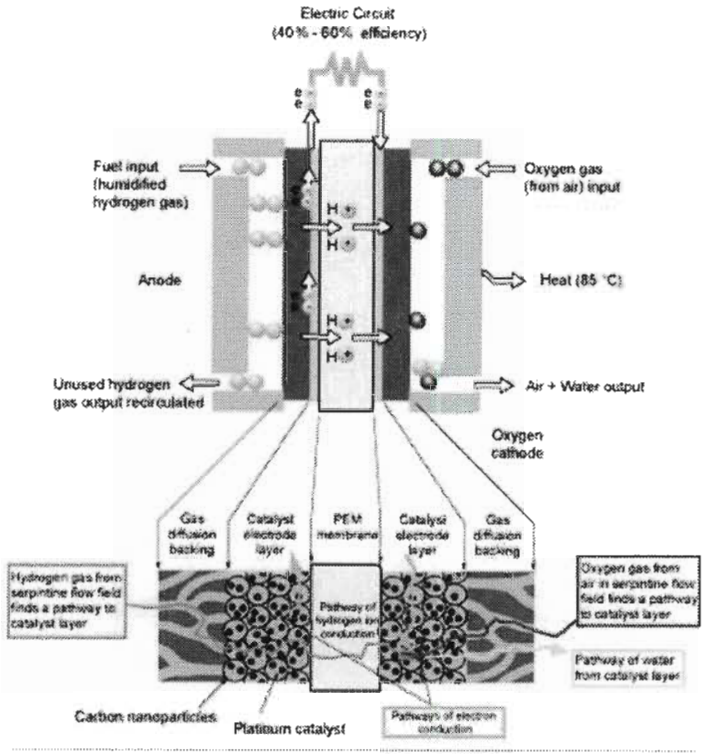

Figure 1-5. Schematic of a single typical proton exchange membrane fuel cell[16]

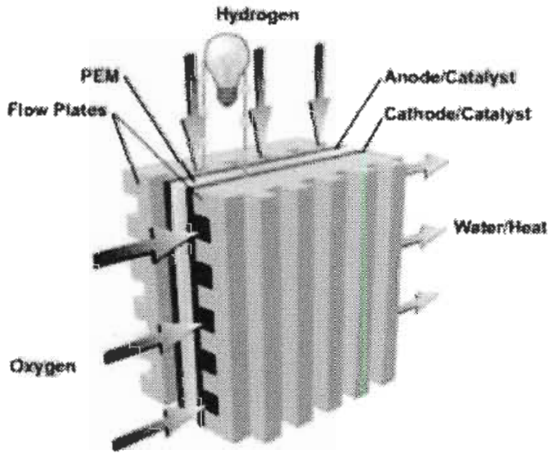

Figure 1-6. Structure and principle of proton exchange membrane fuel cell[17]

Figure 1-6 is the intuitive diagram of a single PEMFC. Hydrogen in the anode meets the oxygen in the cathode at the proton exchange membrane in the interlayer between the electrodes. Then electricity will be produced and transported into the circuit. Heat and water will be exhausted as the byproducts. Then, the unused hydrogen (mixed in the water) will be exhausted with the water. After recycling and dehydration, the hydrogen

will be reused.

1.1.2.3 Characteristics

Proton exchange membrane fuel cell has following advantages:

The generating process does not involve hydrogen combustion. Thus, it is not limited by the Carnot cycle and improves energy conversion rate. In the process of power generating, there is almost "0" pollution noise. Generating units is integrated, Therefore, this generating system is modular and high reliability.. At the same time, maintenance and assembly are very convenient. Therefore, this power is a green power which is clean and efficient.

Typically, the operating of PEMFC requires a series of auxiliary equipments which constitutes the generating system. The generating system of PEMFC consists of the stack, hydrogen supply systems, water and heat management systems, power conversion, control systems and other. The stack system is the core of generating systems. PEMFC has some obvious advantages such as: low temperature, fast starting, simple structure and easy operating[18][19].

1.1.2.4 Application

After many years of researching and application developing, PEMFC has already got the substantial progress for automotive power. Miniature and small portable PEMFC and has reached giant achievements. Additionally, medium and large PEMFC power generating system has also achieved some results. Since the PEMFC is expired to become the main development direction in mobile equipment, backup power supply and some special buildings[20]. In the study of alternate hydrogen power systems, the researching is not only being focused on the fuel cells. The stack quality, efficiency and reliability are also important in the application which includes:

1. integration technology of the generator

2. fuel cells' adaptability to the environment
3. output compensation and power conversion technology
4. parallel operating and controlling of the generator
5. alternate hydrogen and hydrogen storage
6. air (oxygen) supplying
7. hydrogen monitoring and emission
8. development of automation equipment and control systems in hydrogen power plant
9. construction of the power plant and some other application[21]

1.1.3 Electric vehicle

Electric vehicle (EV) is a vehicle which uses the automotive battery as its power to drives wheels by the electric motor. As a vehicle, it also needs to follow the road specifications, safety regulations and other transportation requirements. Compared with the conventional cars, the electric vehicles impact environment fewer. Thus, its prospects are promising widely.

In their power systems, electric vehicles can be classified to: pure electric vehicles (EV), hybrid electric vehicle (PHEV) and fuel cell vehicles (FCEV)[22].

1.1.3.1 Pure electric vehicles (EV)

Pure electric vehicle is the vehicle which is driven by eclectic motor. Its power comes from a rechargeable battery or other energy storage devices.

Most of the EVs are directly driven by motor which is installed in the engine compartments. However, some vehicles use the four wheels motors. The difficulty is the power storage technologies. The electric vehicle does not emit harmful gases into the atmosphere. However, the electricity to charge the vehicle is mostly come from the thermal power station and little part come from hydropower or other source. The electricity for charging can be obtained from some renewable resources such as: hydro,

Rapport-Gratuit.com

wind, solar, heat, etc. It and temporarily relieve the lacking of fossil energy resources. Undoubtedly, the pure electric vehicles are the excellent transitional technology.

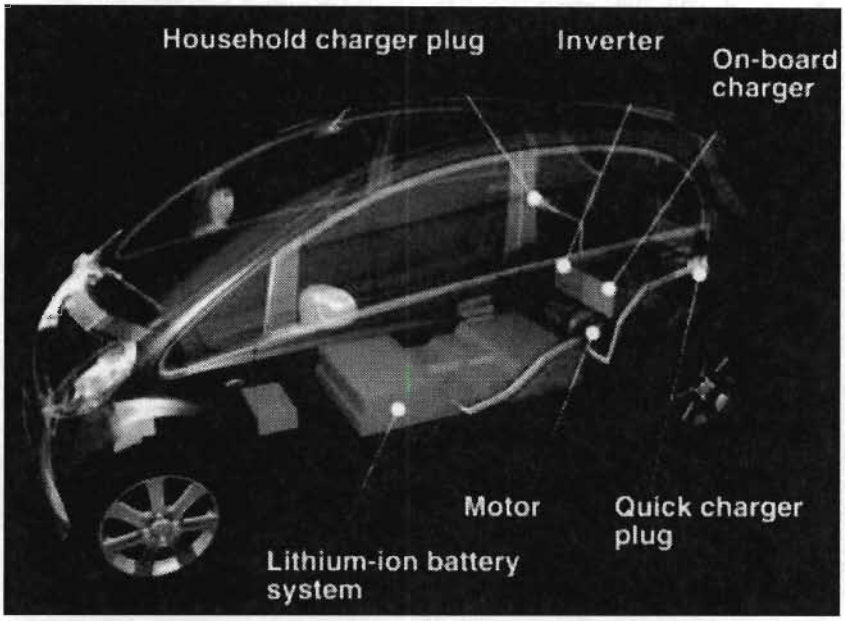

Figure 1-7. Full electric vehicle and the charging device[23]

Advantages: Technology is mature and relatively simple. Wherever there is power supply, the vehicles can be charged.

Disadvantages: Energy storage of battery (per unit weight) is relatively small. The price of battery is expensive which will cause the cost of operating higher than some normal vehicles. It mainly depends on the life of the battery and the prices of local gas and electricity.

1.1.3.2 Hybrid electric vehicle (PHEV)

PHEV is the vehicle which is able to obtain power from at least two of the following types (in Figure 1-8). (According to the form of system structure, the power can be divided into the following four categories):

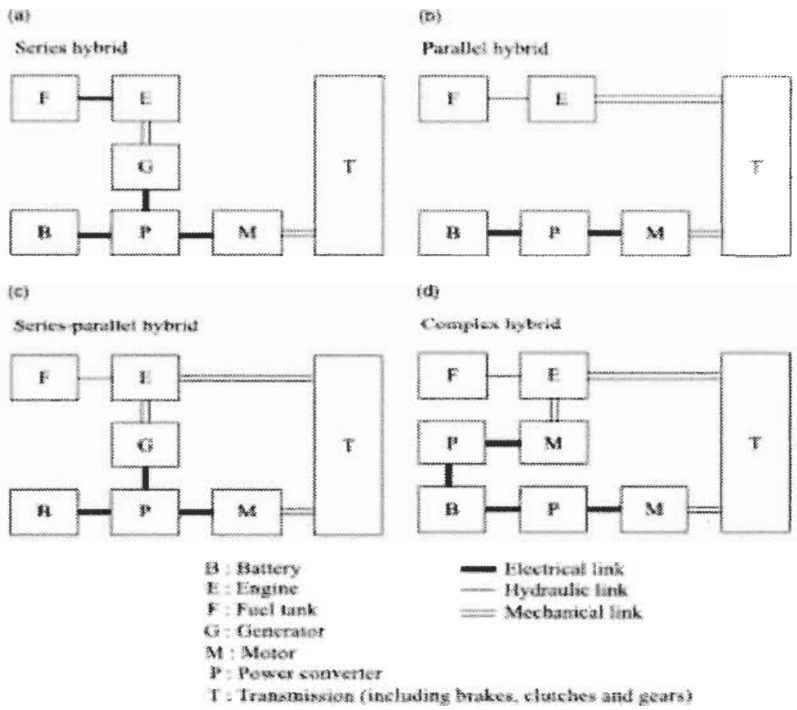

Figure 1-8. Classification of different type hybrid electric vehicles[24][25]

Series hybrid electric vehicle (SHEV): SHEV is the vehicle whose driving force only comes from the hybrid motor (electric). Its characteristic of structure is that the generating motor drives generator and supplies the power. Power is delivered to the electric motor through the controller and drives the vehicle[25].

Parallel hybrid electric vehicle (PHEV): PHEV is the hybrid electric vehicle whose driving force is supplied by the electric motor and the engine simultaneously or independently. Its characteristic of structure is that the parallel drive system could not only use motor or engine independently as its power source, but also can use a motor and engine simultaneously as its power source to drive the vehicle[26][27].

Series-Parallel hybrid electric vehicle (SPHEV): according to its name, this structure is a combination of series and parallel principles. This combination can provide more flexibility at the cost of increased complexity. This is a parallel arrangement where the heat engine is connected to an electrical generator. Then, the management system will easily control the amount of torque to move the wheels. However, the high operating and

Rapport-gratuit.com
LE NUMERO 1 MONDIAL DU MÉMOIRES

maintenance cost is its disadvantage[25].

Complex hybrid electric vehicle (CHEV): CHEV is the vehicle which both possesses series and parallel mode of driving. Its characteristic of structure is that it could work not only in series mode but also in parallel mode[25].

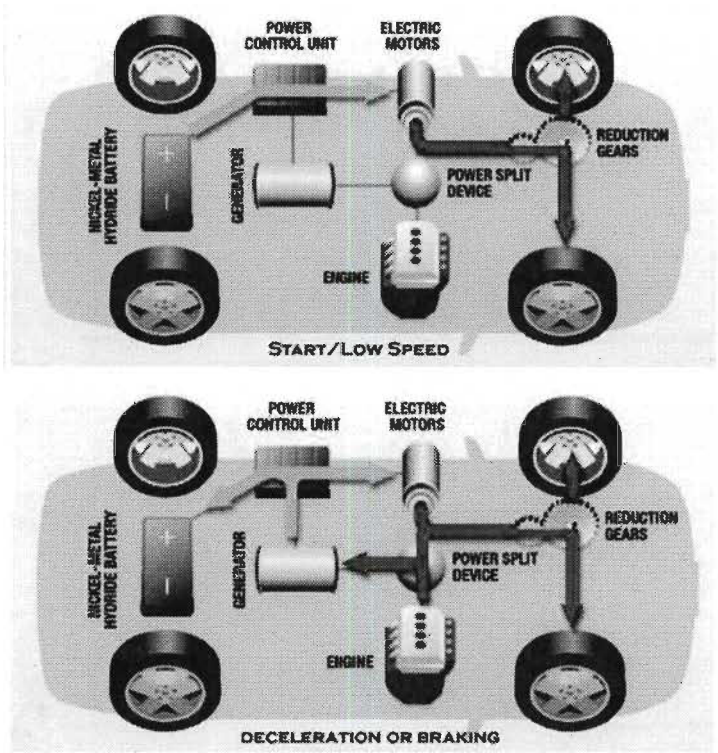

Figure 1-9.Hybrid electric vehicle[28]

Advantages:

1. After using the hybrid power mode, vehicle can determine the maximum power of the engine according to the average requirement. In this case, the fuel consumption and the pollution are low. When the vehicle needs to accelerate but the power is insufficient, battery will supply it. While the load is low, the surplus power can generate electricity to charge the battery. In the operating process, the internal combustion engine could operate continuously if the fuel is enough. Then the battery can be charged continually. So its endurance is equal to the normal vehicle.
2. With the participation of battery, the energy can be easily recovered after some situation such as: braking, downhill and idle speed.

3. In city, the engine could be switch off and the vehicle will be driven by battery independently in order to achieve "zero local".
4. With the internal combustion engine, the problems of energy consumption such as air conditioning, heating, and illumination which the pure electric vehicle faces could be easily solved.
5. Refueling can be finished in the existing gas station and the more reinvest is unnecessary.
6. Complex hybrid technologies can keep the battery in good working condition. It avoids over charging-discharging which could extend battery life and reduces costs.

1.1.3.3 Fuel cell electric vehicles (FCEV)

A fuel cell electric vehicle uses the fuel cell as its generator which can charge the battery in the running process. Chemical reaction process of the fuel cell does not produce harmful products. Therefore, it can be called non-polluting vehicle. The energy conversion efficiency of the fuel cell is 2-3 times higher than the internal combustion engine. On the hand of environmental protection, fuel cell vehicle is an ideal vehicle. Individual fuel cells must be integrated into a fuel cell stack, in order to obtain the necessary power to meet the requirements of the vehicles. In the development of fuel cell vehicle, technical challenges are still exist such as: integrating the fuel cell stack, improving the commercialization of fuel processors, manufacturing of automobile accessory, integrating components and others.

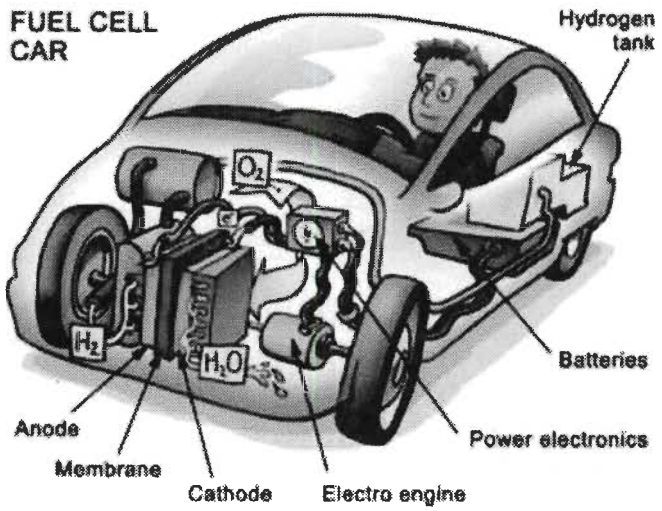

Figure 1-10.The concept model of fuel cell electric vehicles[29]

Comparing with ordinary internal combustion engine vehicle, fuel cell vehicle has the following advantages:

1. It is zero local or approximately zero local.
2. There will be no water pollution caused by oil leakage.
3. It can reduce the emissions of greenhouse gas.
4. Fuel economy and efficiency of engine combustion will be improved.
5. It runs smoothly with no noise.

1.2 Introduction of the devices

1.2.1 Nemo-fuel cell electric vehicle

Nowadays, vehicle exhausting acts a main part in the "Greenhouse Gas" emission which caused serious affect in the environment. In order to solve these environment problems, the electric vehicles including Hybrid Electric Vehicles (HEV) and Battery Vehicles (BV)[30] gradually replace the internal engine vehicles. However, the HEV is still indivisible with the oil industry and its future is not optimistic. On the other hand, BV doesn't act very satisfactory while being compared with the HEV[31].

Summing up the above advantages and disadvantages, Fuel Cell Vehicle becomes the

most advantageous candidate because of its zero local, high energy efficiency and fast recharging[32].

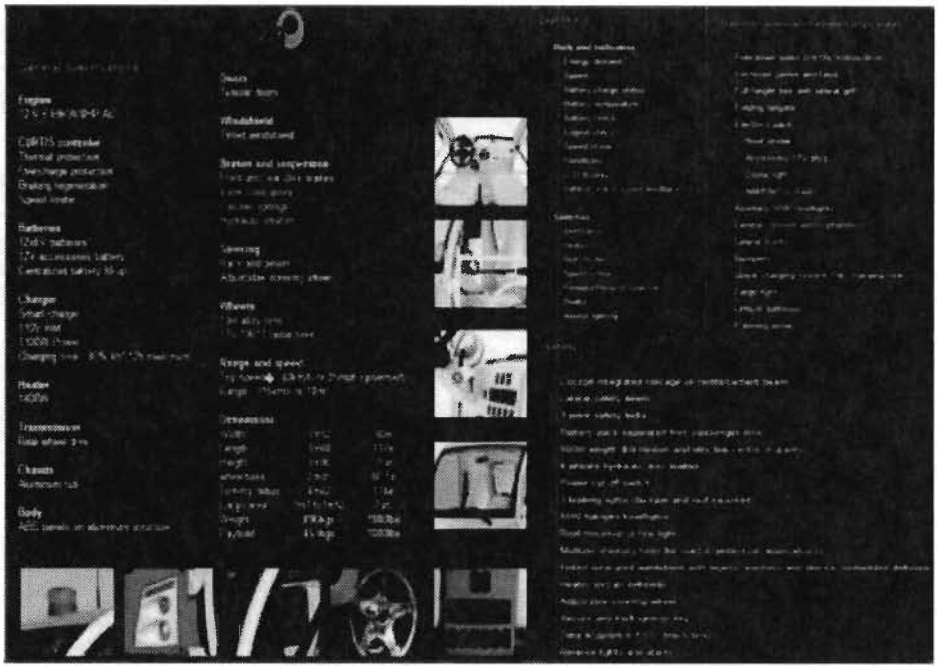

Figure 1-11.Characteristic and parameters of Nemo electric truck[33]

Nemo is a low speed fuel cell vehicle (LSV) which can give a high loading and torque. (Figure 1-11 & Figure 1-12)

Figure 1-12.Exterior and interior of Nemo

In order to improve Nemo's endurance and solve the problem of its power source, the integrating PEM fuel cell produced by Axane® is equipped in the vehicle. This designing and modification is made in IRH (Institut de recherche sur l'hydrogène). Further research is continued in the institute including the embedded systems and the optimization of the

vehicle, battery, and fuel cell. The original parameters are shown in Table 1-2.

Table 1-2. Original specifications of Nemo truck

Parameters of The Nemo	
Dimensions	
L: W: H	3.48m:1.52m:1.90m
Tires	175/70R13
Weight	896kg
Maximum Load	453kg
Driving Performance	
Maximum Speed	40km/h
Acceleration	6.5s (0-Max)
Autonomy	115km
Transmission	
Engine	ACX-2043;4.8kW
Transmission Report	12;44:1
Batteries	
Battery series	9X8V U.S battery®
Battery Type	Lead-acid deep cycle
Battery charger	1.3kW

1.2.2 Basic principles of the Nemo

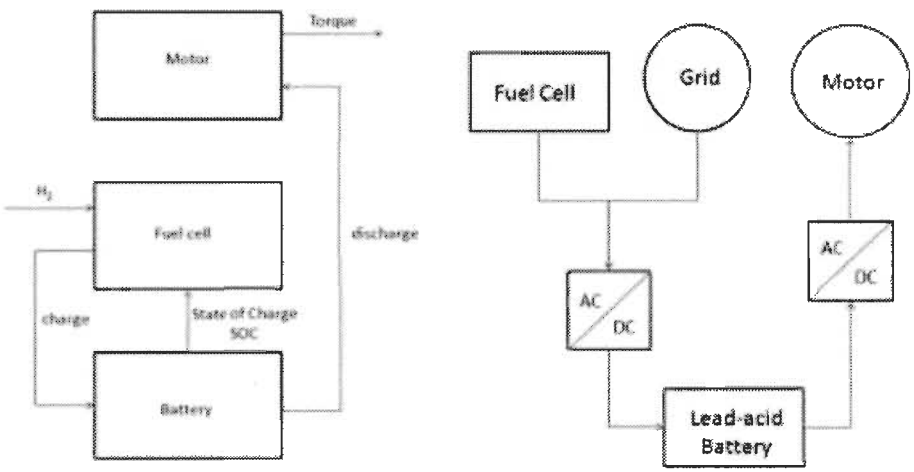

Figure 1-13. System model of Nemo HEV

In Figure 1-13, it shows the system model of the Nemo. The driving power is given by the electric motor. The function of the battery is to support the electric power to the motor.

When the state of charge (SOC) is lower than the set depth of discharge (DOD), the generator will be switched on to charge the battery. Therefore, the PEMFC acts as the generator in this system.

1.2.3 Utilization of battery series

Figure 1-14. 8V deep cycle U.S Battery[34]

Nemo uses the 9 series 8V U.S batteries as its power source. This type of batteries is the most suitable candidate for the golf cart and multi-propose vehicle. Its feature is fully complying with Nemo's request for carrying the freight or mounting trailer and other applications. In the 8V U.S battery series, there are three productions: 8VGC XC2; 8VGCHC XC2 and 8VGCE XC2.

Among the three productions, the "US 8VGCHC XC2" battery is chosen to be installed in Nemo because of its high capacity which can drive Nemo for a longer distance.(parameters are compared in Table 1-3 [35]. Additionally, the 8V series battery has a marvelous performance on its output power which can help the vehicle quickly start and accelerate.

Table 1-3. Parameters of 8V U.S Battery

U.S. Battery Model	Amp Hours (20 hr. rate)	5 hr rate	M.C.A. @32F	Minutes @ 75 Amps	Minutes @ 25 Amps	Length	Width	Height	Cover and Case	Pallet Qty
US 8VGC XC2	170	138	128 minutes	90	337	10 1/4" (260mm)	7 1/8" (181mm)	11 1/4" (286mm)	RED/WHT	48
US 8VGCHC XC2	183	141	136 minutes @ 56 amp	95	345	10 1/4" (260mm)	7 1/8" (181mm)	11 1/4" (286mm)	BLU/WHT	48
US 8VGCE XC2	121	101	90 minutes @ 56 amp	60	230	10 1/4" (260mm)	7 1/8" (181mm)	11 1/4" (286mm)	BLK/WHT	48

1.2.4 Utilization of PEMFC

Figure 1-15. AXANE® PEMFC[36]

The 48 series PEMFC which produced by Axane® is the energy support of the Nemo truck and they are used to charge the battery. Therefore, the energy exchanging between fuel cell and battery is the pure electrical energy conversion.

Axane® designed and made fuel cells for different uses, such as emergency backup generators. For example, it can be used when the power grid is not reliable or if it becomes unavailable[37].

The parameters of PEMFC which is equipped on the NEMO are given in Table 1-4.

Table 1-4. Parameters of Axane® PEMFC

Parameters of Fuel cell	
Company	Axane®
Power (W)	2500
Max Voltage (V)	48
Max Current (A)	52
Temperature (°C)	1-45
Hydrogen pressure (bar)	1.25
Air pressure (bar)	1.013
Weight (kg)	82

Normally, the price of fuel cell depends on its power (280$/kW)[38]. However, as a fuel cell which is used for the researching experiment, the price is not comparable. The cost of Axane® PEMFC should be discussed under special conditions. Therefore, in this work, the cost of fuel cell refers to the commercialized fuel cell.

1.3 Chapter summary

In this chapter, the classifications and features of some species of fuel cells are introduced. The electrical vehicles are also presented including their system structures (series and parallel) and reload methods (refueling or charging).

The proton exchange membrane fuel cell is the emphasis of the study because of its low operating temperature. It is the best candidate of automotive fuel cell. The Nemo truck, which is being optimized in "L'Institut de recherche sur l'hydrogène (IRH)" is a low speed vehicle and with incredible solid dependability and flexibility.

Rapport-Gratuit.com

The parameters of Nemo are given in this chapter. The other devices which are used in the Nemo are also introduced. By the control system, the dynamic module, the fuel cell module and the battery module are linked. The objective of this work is to optimize the operating cost through comprehensively analyzing the consumption of each module.

Chapter 2 - Current Situation and Expected Optimization

The existing optimizations for the Nemo truck have achieved certain results. The two energy managements (energy managements for the fuel cell and energy managements for the battery) which are related to this work are described. Continually, the optimization method which is used in this work is introduced. Economic optimization for hydrogen cost and battery cost is the main purpose of this work.

2.1 Existing optimization

Nemo is a battery vehicle which is modified to be a hybrid electric vehicle in IRH-UQTR. To improve its endurance, energy saving and environment protection, a 2.5kW proton exchange membrane fuel cell and a 5kW internal combustion engine generator are both installed. The objective of optimization is to get rid of the fossil fuel gradually under the premise of its work stability. To ameliorate the performance of the vehicle, energy efficiency is the most important factor. Not only in the fuel cell system but also in the battery system, the energy management control is the effective method to increase the fuel efficiency.

2.1.1 Energy management of fuel cell

Figure 2-1 reflects the energy distribution in the fuel cell. The energy occupation of the air supply is 25% and second only to the electric load. To increase the energy efficiency, a air compressor is used to solve this problem[39].

Rapport-gratuit.com
LE NUMERO 1 MONDIAL DU MÉMOIRES

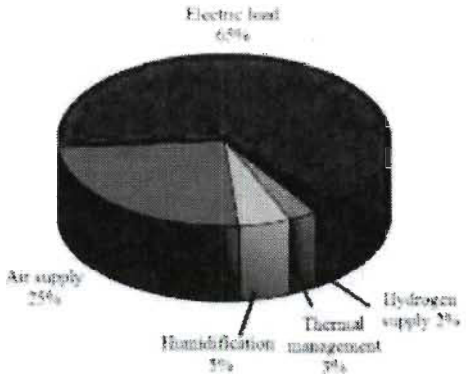

Figure 2-1. Energy distribution in the fuel cell[39]

This optimization is to obtain an air supply with a compressor or an air pump. In a fuel cell, air supply acts very important[40]. Result by its inner energy consumption, it affects the quality of the energy conversion and efficiency in the fuel cell stack. There is a problem which is often been neglected. That is on the water management, the gas supply has an important impact. Therefore, the accuracy of the energy management control is highly required.

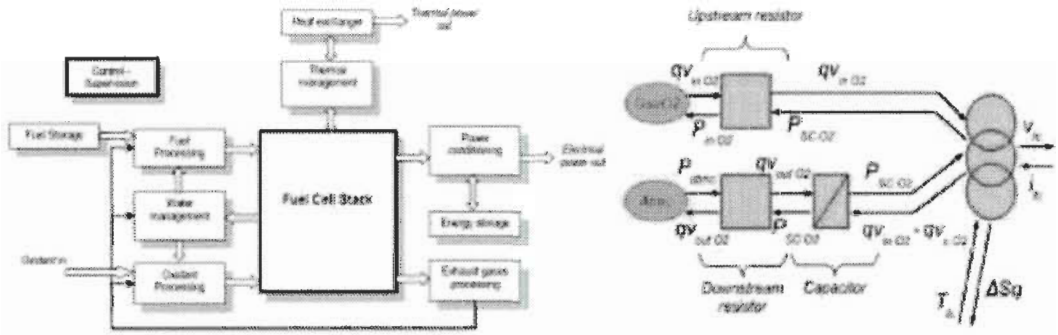

Figure 2-2. Synoptic of a fuel cell system and the model of the air supply management system[39]

A fuel cell system is a multi-physics energy converter which implies electricity, thermodynamics, fluidic and electrochemistry. This method is most focusing on the humidity management and the influence of the air supply management as the output of the fuel cell stack which is shown in Figure 2-2. Additionally, by using a real time control loop to improve the air supply energy management, a first indicator of the quality of the

water management has been presented.

Through the method of adding in the air compressor, a significant result of the first analysis for the energy management is provided. The future work can be begun by the designing of an efficient air supply control strategy which should be aided by the fuzzy logic.

2.1.2 Energy management of battery

The power management strategy optimization has been done and the battery life cycles and the aging model are included[41]. To improve the Nemo from BV to HEV, the modification is shown in Figure 2-3 :

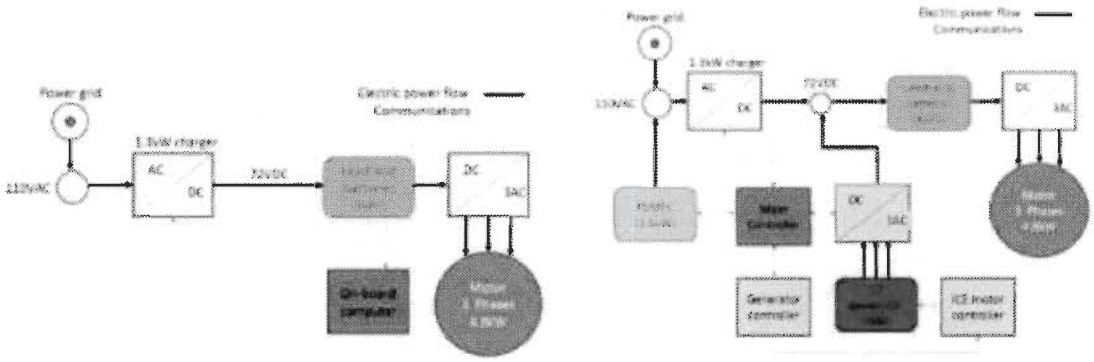

Figure 2-3. Original Nemo EV architecture and modified Nemo HEV architecture[41]

When being parked, the charging power is provided by the grid. PEMFC and internal combustion engine generator will be started while driving.

As the figure shows, PEMFC is added into the operating circuit as the power resource. At the same time, internal combustion engine generator also works in another power provision branch as its alternate power when the fuel (hydrogen) in tank is empty. The alternating current is supplied by the ICE generator. Therefore, the Lead-acid battery will be charged by the direct current while the DC-AC converter is set between the generator and battery. Both of the direct current will be controlled by the main controller. The block diagram is presented as:

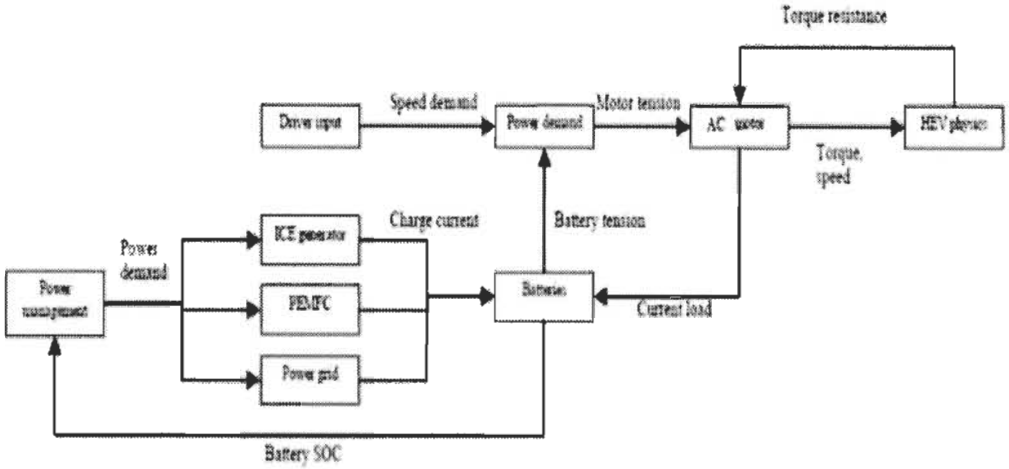

Figure 2-4. Block diagram of the Nemo[41]

The two driving charging systems can work independently. Therefore, the optimization will be only focused on the branch of the PEMFC charging circuit and the flow chart is shown in Figure 2-5 :

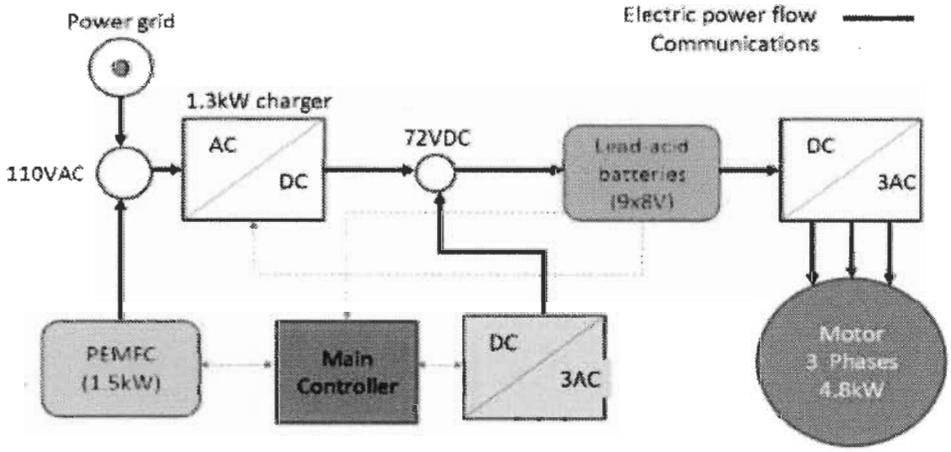

Figure 2-5. Charging circuit of PEMFC-battery[41]

2.2 Objective and expected optimization - Energy management of charging system

Fuel Cell acts as a converter of energy exchanging between electric and chemical. This electro-chemical reaction between hydrogen and oxygen produces electricity, water and heat[42]. By adjusting the operating parameters, such as temperature, switching time and drag, the best operating status will be found which is called "optimization" [32]. This

work presents the methods of efficient management and the optimization of consumption. By using these methods, the utilization of fuel (hydrogen) and the cost caused by the battery life will be improved.

Another factor which cannot be ignored is the energy consumption of the charging circuit. In other word, the charging form and the charging efficiency are important factors because charging the battery is the purely conversion from chemical energy to electrical energy (appending with thermal consumption). At the same time, the battery life is also significantly affected by the charging methods. Consequently, the energy management of charging circuit will directly affect the operating cost of battery. Some effective charging methods are used to achieve the goal, such as trickle charging and constant voltage charging.

In this optimization work, the variable resistor is added in the charging circuit. The charging efficiency is increased and the consumption of the fuel and the battery life will be effectively improved.

2.2.1 Flow chart of Nemo truck

Evolving from the model in Figure 2-5, the logical relationship among each parts of the Nemo's system is expressed in Figure 2-6:

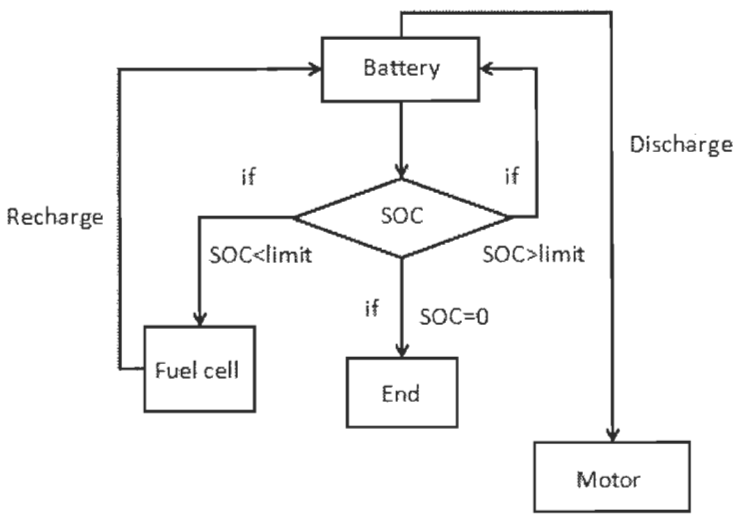

Figure 2-6. Flowchart of Nemo's operating principle

In Nemo truck, battery supports the power to the electric motor directly. Therefore, the state of charge is the monitor of the total model. The Nemo uses 9 series "American Battery®" 8&12 volt battery as its power source. Because of the high price of battery (200$/single battery), to find a balance point (SOC limit) between the cost of battery and hydrogen is the aim of optimization.

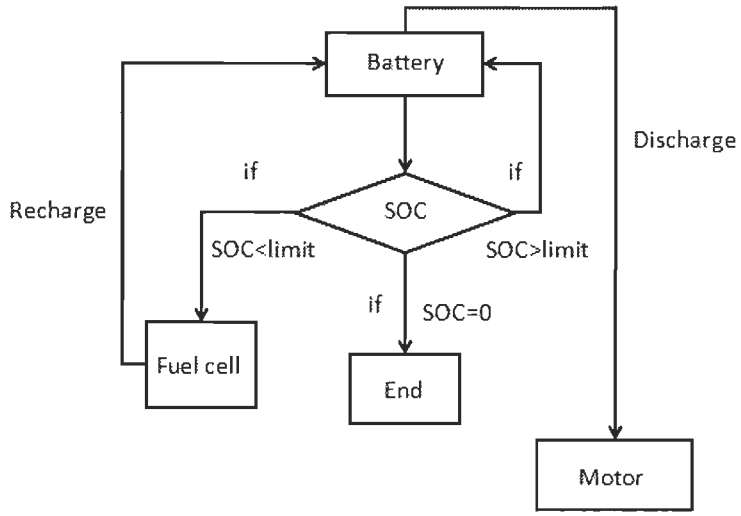

As Figure **2-6** shows, if the SOC is higher than the set limit, the fuel cell is off. While the SOC is lower than the set limit, fuel cell will be switched on to charge the battery. Else, when hydrogen in tank is empty, there will be no chemical energy for the fuel cell to produce electricity. With the continued operating, SOC will tend to 0%. At this time, the total system (including the fuel cell, the vehicle and the battery) will stop[43].

2.2.2 Battery status

To reflect the status of battery, there are two parameters: Depth of Discharge (DOD) and State of Charge (SOC).

In the operating of battery, the percentage of battery capacity release is called the depth of discharge (DOD). The level of DOD concerned with the life of secondary batteries (rechargeable storage battery or battery).The deeper the depth of discharge is, the shorter the battery's life will be. Therefore, deep discharging should be avoided in operating.

State of Charge (SOC) is the remaining power in the battery. It is the important monitor to

reflect the status of the remaining power in the battery and especially in the electric vehicle. The function of SOC is same as the fuel gauge in the internal combustion engine vehicles. The measurement of SOC is percent (0% is empty, 100% is full).

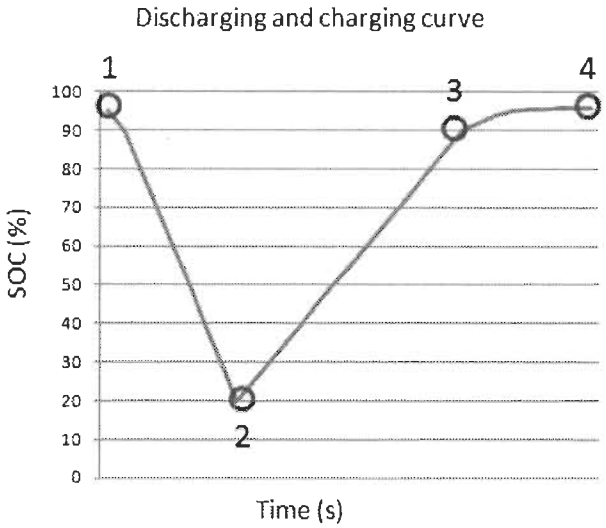

Figure 2-7. Ideal graph of discharging and charging

Figure 2-7 is an ideal graph of discharging and charging, there is no interference in the process of discharging and charging. Point 1 is the beginning of discharging and the SOC decreases continuously. While SOC reaches the limit level (point 2), the fuel cell will be started and the motor is turned off at the same time. (Usually, the process of charging is longer than the process of discharging because the output power is larger than the input power.). When SOC is charged to a certain level (point 3), the charging rate decreases obviously because of the aging phenomenon of battery. Generally, the fuel cell can be switched off at this time because the charging efficiency is very low. If continue to charge, the SOC will rise till the full status (point 4).

Theoretically, in a single battery, the maximum of charging level is about 95%. When the SOC reaches this level, the charging efficiency will decrease significantly. Therefore, in the operating of Nemo, the maximum charging level is set at 95%. Thus, the unnecessarily wasting of hydrogen can be avoided. In operating, DOD and SOC are antithetical parameters (DOD+SOC=100%) which is shown in Figure 2-8.

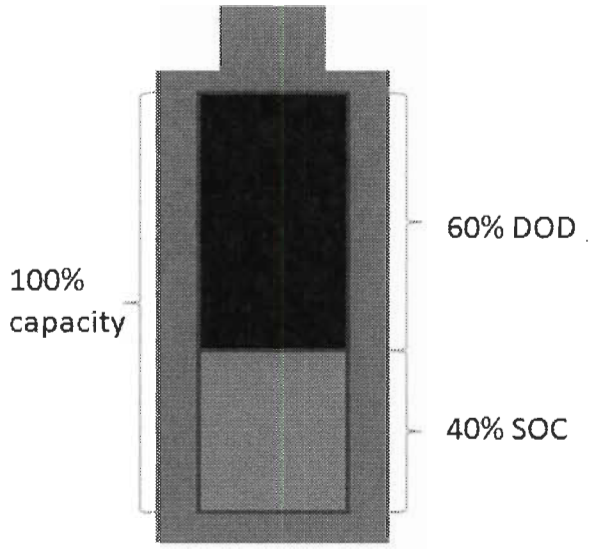

Figure 2-8. Capacity of battery status

2.2.3 Cycles of battery charging

A charge cycle is the process of discharging a rechargeable battery and charges it. The term is typically used to specify a battery's expected life, as the number of charge cycles affects life more than the process time. Discharging the battery fully before recharging is called "deep discharge"; partially discharging then recharging may be called "shallow discharge".

In general, number of cycles for a rechargeable battery indicates how many times it can undergo the process of complete charging and discharging until failure or it is starting to lose capacity[44].

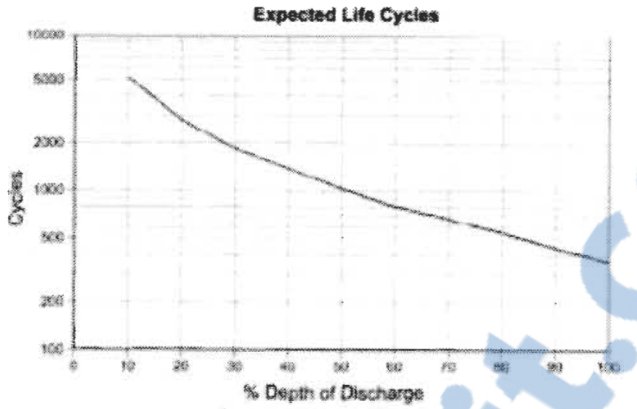

Figure 2-9.Relationship between depth of discharge and life cycles of battery[46]

Figure 2-9 is constructed for a Lead acid battery. The trend of curve is caused by the principle that battery life depends on the total energy throughput that the active chemicals can tolerate. Ignoring the battery aging phenomenon, the total energy is fixed. (It can be regarded that 1 cycle (100% DOD) ≈ 2 cycles (50% DOD) ≈ 10 cycles (10% DOD) ≈ 100 cycles (1% DOD)). Therefore, for the chemical battery, the aging effects are the main cause of the battery cycles life[45].

2.2.4 Aging cost of fuel cell system

For the fuel cell system, the cost is depending on the degradation of the system itself.

$$Cost_{fuel\ cell} = \frac{Power_f \times Price_f}{Life_f} \times t \qquad (2.1)$$

In the Nemo truck,

$Power_f = 2.5kW$

$Price_f = 280\$/kW$[38]

$Life_f = 2{,}000 - 2{,}500\ hours$

Then, the cost of fuel cell is 0.28-0.35$/hour.

In this work, the operating time is constant value. Therefore, as a fixed value, the cost of

Rapport-Gratuit.com

fuel cell system will not be taken into account in the optimization.

2.2.5 Cost of battery

Equation (2.2) is the expression of the battery. It is determined by several factors: output power of battery, available charging cycles, numbers of battery series and the charging cycles in the operating process.

$$Cost_{battery} = \frac{P_B}{L_B} \times C_{ch} \times n_B \tag{2.2}$$

Here,

$\boldsymbol{P_B} = single\ battery\ price$

$\boldsymbol{L_B} = life\ of\ battery$

$\boldsymbol{C_{Ch}} = charging\ cycles\ during\ the\ operating\ process$

$\boldsymbol{n_B} = number\ of\ batteries$

The relationship between the battery life and the depth of discharge appears to be logarithmic as shown in Figure 2-9. In other words, the number of cycles yielded by a battery goes up exponentially the shallower the depth of discharge(DOD)[47].

Normally, each species of battery has its own relationship curve between the charging cycles and the depth of discharge. However, the track of curves is usually similar.

2.2.6 Present hydrogen consumption of fuel cell

The presently hydrogen consumption is reported in Figure 2-10. This result comes from the dynamic simulation of the Nemo. In the simulation process, the total test time is 137000 second (100 UDDS loops; 1 UDDS loop consumes 1370 seconds). Throughout the process, the charging cycles of battery is 55.

To calculate the consumption, the relationship is presented as equation (2.3)

$$Cost_{hydrogen} = (\frac{I_{ch} \times n_f}{2F} \times \eta) \times (t_1 - t_0) \times A_{cost}$$

(2.3)

In the equation,

$\boldsymbol{t_1} = \textit{the ending time of the operating process}$

$\boldsymbol{t_0} = \textit{the starting time of the fuel cell}$

$\boldsymbol{I_{ch}} = \textit{charging current } (A)$

$\boldsymbol{n_f} = \textit{the number of fuel cell series}$

$\boldsymbol{\eta} = \textit{Faraday efficiency of fuel cell}$

$\boldsymbol{F} = \textit{the faraday constant } (96{,}485.3365\ C/mol)$

$\boldsymbol{A_{cost}} = \textit{price conversion of hydrogen } (\$/mol \rightarrow \$/kg)$

The result of the simulation is shown in Figure 2-10:

SOC (%)	H2 Kg/100km
0	0.485
5	0.497
10	0.508
15	0.519
20	0.529
25	0.54
30	0.55
35	0.561
40	0.517
45	0.582
50	0.592
55	0.602
60	0.613
65	0.624
70	0.634
75	0.645
80	0.655
85	0.666
90	0.676
95	0.687
100	0.7

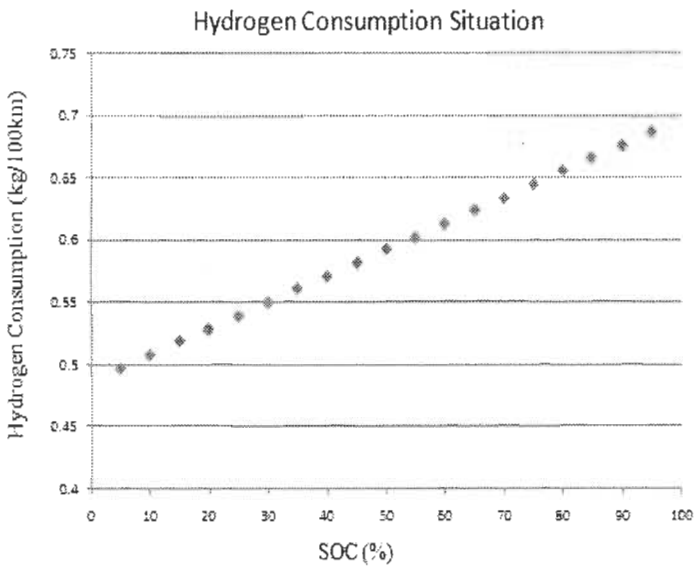

Figure 2-10.Hydrogen charging consumption curve from SOC 0%-100%

While switching on the fuel cell at 0% SOC (the minimum requirements of SOC) to charge the battery till the end of the process, the consumption of hydrogen is 0.485

Rapport-gratuit.com
LE NUMERO 1 MONDIAL DU MÉMOIRES

kg/100km. In this case, hydrogen consumes minimally. Conversely, if the fuel cell is switched on at 100% of SOC(Theoretically, the maximum SOC is 100% and the max level is continually reducing because of the aging of the battery) and the battery is being continually charged while the vehicle is started[25]. In this case, hydrogen consumes maximally and the amount is 0.7 kg/100km.

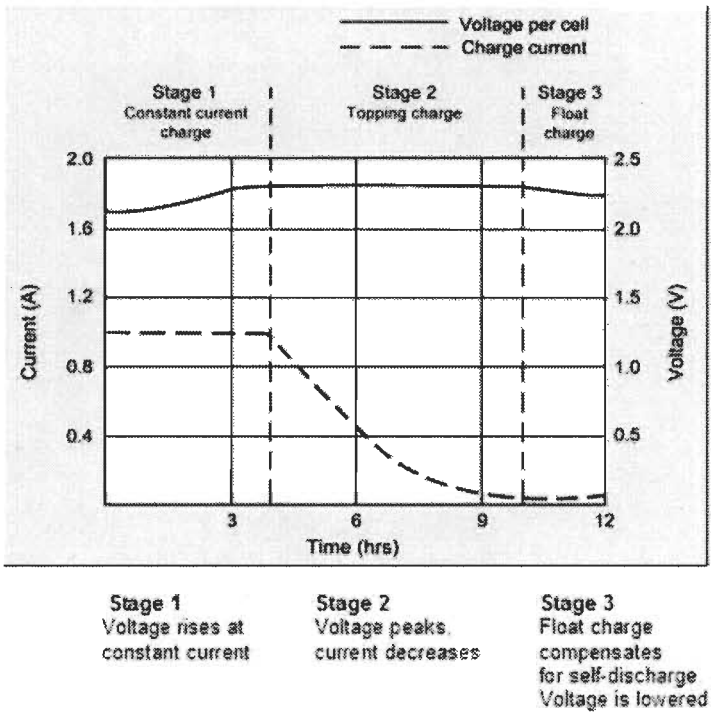

Figure 2-11. Charging efficiency and SOC in different charging stages[48]

Firstly, starting charge at a high SOC level will cause the extending of charging time. Additionally, the charging process is kept at the status of topping charge or float charge. In these charging stages (according to Figure 2-11), the charging efficiency is low and the fuel efficiency is reduced.

Even though, charging battery at a high SOC level will increase the available charging cycles of battery. However, more hydrogen will be consumed because of the low fuel efficiency.

2.2.7 Cost economization

Comprehensively consider with the price of the battery and the hydrogen, early charging

will consume more hydrogen, and delay charging will cause the charge depth too high[49], which affects the life of the battery obviously. Thus, through this phenomenon, the relationship curve will be generally as the following figure shows:

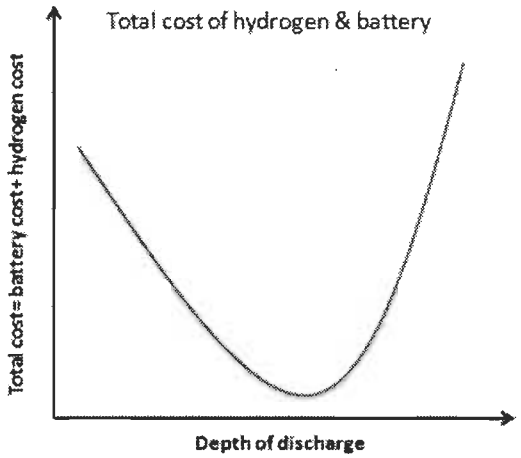

Figure 2-12. Curve of the operating cost

$$Cost_{total} = Cost_{hydrogen} + Cost_{battery} + Cost_{fuel\ cell}$$

(2.4)

The curve is the sum of the battery, hydrogen, and the fuel cell cost. From the analysis of the curve, the purpose of optimization is to minimize the total cost. Obviously, the objective of the work is to find the best time to start the fuel cell which can make the total cost lowest.

The following expression presents the sum:

$$Cost_{total} = \left(\frac{I_{ch} \times n_f}{2F} \times \eta\right) \times (t_1 - t_0) \times A_{cost} + \frac{P_B}{L_B} \times C_{Ch} \times n_B + \frac{Power_f \times Price_f}{Life_f} \times (t_1 - t_0)$$

(2.5)

2.3 Chapter summary

In this chapter, the existing optimizations are introduced: the energy management of fuel

cell and the energy management of battery. Furthermore, the new optimization focusing on the charging method is given including the charging time and the charging circuit. The optimization of charging time is to find the most appropriate time point to start the fuel cell for charging battery. "Appropriate" means starting fuel cell during this period, the operating cost will be minimized. Through summarize the cost of each part; the lowest consumption will be the optimization.

Chapter 3 - Simulation

Matlab is the main simulation tool for this work. By comprehensively simulating the three model of the Nemo truck (dynamic model, battery model and fuel cell model), the final consumption can be calculated. Though the result of simulation, the optimization for the total cost could be designed and implemented.

3.1 Basic model of Nemo truck

$$P_{output} = P_{torque} = P_{battery} \tag{3.1}$$

When operating, battery supports the required power of motor. If the fuel cells are not installed, the power of final output is equal to the battery power. Therefore, the power of the battery capacity is mostly transferred to be the mechanical power. A little part of the chemical energy produces heat. This is the operating mode of pure battery vehicle and its endurance only depends on the capacity of the battery[54]. In this case, as the hybrid electric vehicle, the Nemo's target is to solve the problem of low endurance. Compressed hydrogen is stored in the tank which is connected to the fuel cell with metal pipe. The function of fuel cell is to charge the battery not only in the process of running but also in the parking period. Then, with the participation of fuel cell, the output power will be presented as following expression:

$$P_{output} = P_{torque} = P_{fuel\ cell} + P_{battery} \tag{3.2}$$

which cannot be ignored is the heat which is produced in the battery's discharging process and the fuel cell generating process. Thus, the heat can be considered as the energy loss. Since, the expression is modified as:

$$P_{output} = P_{torque} = P_{fuel\ cell} + P_{battery} - Heat_{fuel\ cell+battery}$$

(3.3)

3.2 Physics and mathematics models of the Nemo

To simulate the operating status of the Nemo, the total vehicle model is composed by three parts: dynamic model, fuel cell model and battery model.

3.2.1 Dynamic model

Running on the road, the process is the confrontation between the power of vehicle and the residences[55].

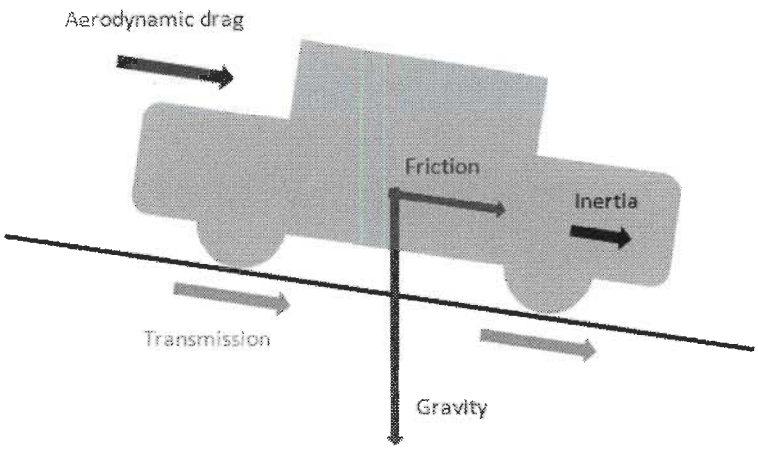

Figure 3-1.The force which was received by the vehicle during the process of driving

The physics model of driving status can be expressed by equation (3.4):

$$F_{torque} = F_{acc} + F_r + F_{ad} + F_{cr}$$

(3.4)

$\boldsymbol{F_{acc}} = \textit{the power of acceleration}$

$\boldsymbol{F_r} = \textit{the friction power of tire}$

$\boldsymbol{F_{ad}} = \textit{the resistance of aerodynamic drag}$

$\boldsymbol{F_{cr}} = \textit{the resistance of climbing}$

And the resistant force is calculated by following equation:

$$F_r = C_{rr} * m_{total} * g * cos\alpha_{slop} \tag{3.5}$$

$\boldsymbol{C_{rr}} = \textit{the coefficient of friction}$

$\boldsymbol{m_{total}} = \textit{the mass of vehicle and fuel cell}$

$\boldsymbol{g} = \textit{the gravity } (9.8N/kg)$

$\boldsymbol{\alpha_{slop}} = \textit{the slop of ground}$

Aerodynamic drag is caused by the flow of air. It is affected mainly by the area of the surface contacting between the vehicle and drag.

$$F_{ad} = 0.5 * \rho_{air} * C_x * A_{aero} * v^2 \tag{3.6}$$

$\boldsymbol{\rho_{air}} = \textit{the density of air}$

$\boldsymbol{C_x} = \textit{the drag coefficient}$

$\boldsymbol{A_{cost}} = \textit{price conversion of hydrogen } (\$/mol \rightarrow \$/kg)$

$$F_{cr} = m * g * sin\alpha_{slop} \tag{3.7}$$

Climbing resistance is affected by the gravity, mass and slop. Due to the gravity and the mass are the constants, the only variety parameter is the slop. While the angle of slop is 0^o, the resistance is 0. Therefore, the climbing resistance exists when the angle slop is $>0^o$ or

$< 0^{o}$. If the angle >0 (down slop), the force of climbing resistance will be positive. On the contrary (up slop), the force will be negative.

3.2.2 Power demand

Driving on the road, the vehicles speed is decided by the accelerator. The accelerator controls the rotational speed directly. Getting rid of the environment affect, the rotational speed increases the acceleration and the brake decreases the speed of vehicles. Actually, all the controlling command is emitted by the driver. Thence, the command is called power demand. Additionally, there is a rule to define the power demand when driving in the city. This rule is the "UDDS" which reflects not only the frequency of accelerating and braking but also the situation of stop and driving at maximum speed.

UDDS is the abbreviation of "Urban Dynamometer Driving Schedule". It refers to the mandated dynamometer test on fuel economy from the institute "United States Environmental Protection Agency "[56]. The test applies only to the light duty vehicle which is driven in the city.

However, Nemo is not a normal household vehicle, but a low-speed truck. Its power demand is different from the normal car and it is changed by its maximum speed (40km/h). Thus, the UDDS is fixed as Figure 3-2 shows:

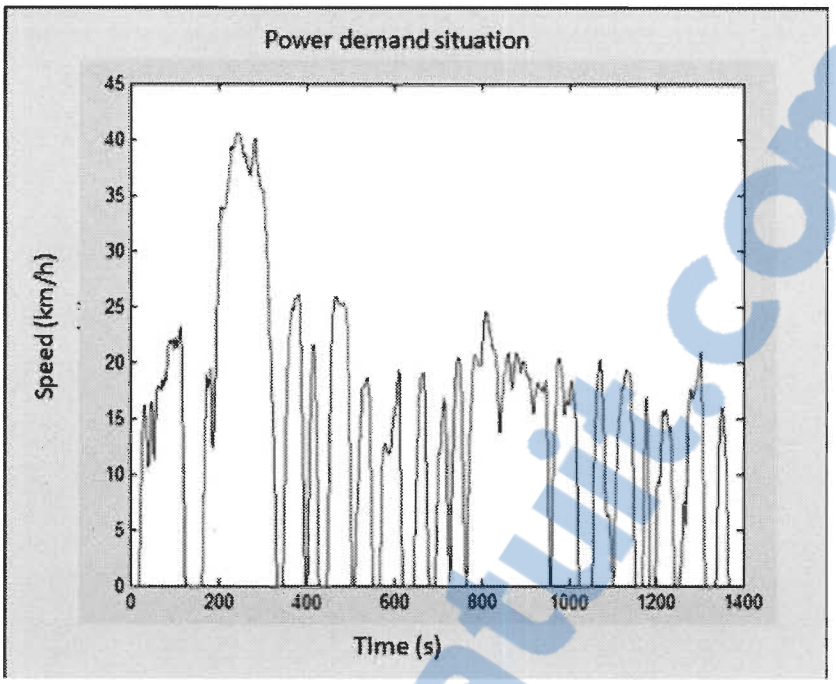

Figure 3-2. UDDS cycle (1370 seconds) of Nemo

Torque is the directly reflect of the power output of the vehicle. It is mainly affected by drag and friction. Here, rolling resistance F_r, aerodynamic drag F_{ad} and climbing resistance F_{cr} are the three variety parameters that should be considered in the dynamic model because they affect the acceleration dv/dt directly. (The parameters are shown in Table 3-1)

Table 3-1. Mechanical operating parameters of Nemo truck

Parameters of NEMO	
Torque	500~2000N
C_{rr} (coefficient of friction)	0.015
ρ_{air} (density of air)	$1.2kg/m^3$
C_x (drag coefficient)	0.42
A_{aero} (area of contact surface)	$4m^2$
m_{total} (mass)	896kg

Rapport-Gratuit.com

In Figure 3-3, it shows the operation status of Nemo. The maximum speed is 12m/s and the acceleration time from the stationary state to the maximum speed is about 20 seconds.

$$F_{acc} = a_{acc}(UDDS) * m \tag{3.8}$$

Additionally, the acceleration depends on the power demand of the operator as Figure 3-2 shows. The cycle of the UDDS continues 1370 seconds; average speed is 23 km/h (6.38 m/s) and the maximum speed is 40km/h (11.8 m/s).

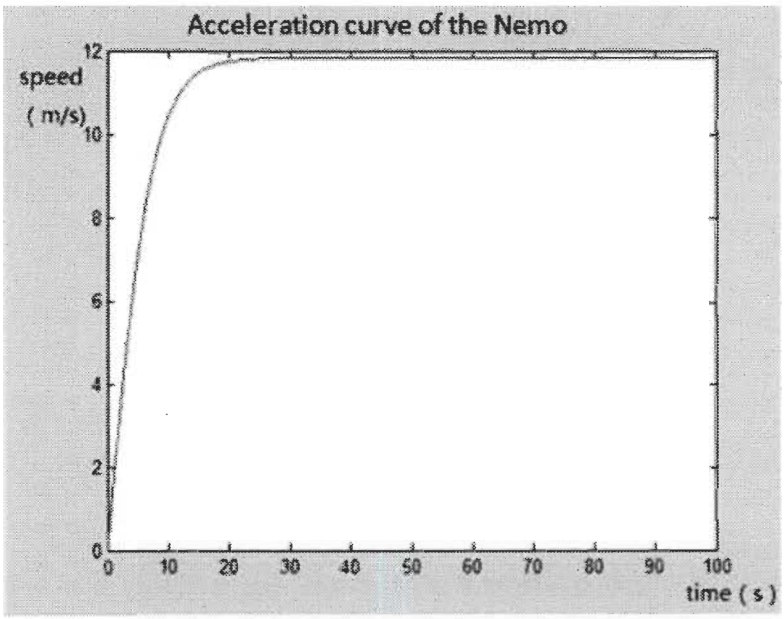

Figure 3-3. Acceleration of the Nemo

3.3 Voltage distribution of fuel Cell

The PEMFC is not a direct battery to drive the electric motor, but acts as the generator on the vehicle. In the operating process, it produces electricity, water and heat. Sometimes, the un-reacted hydrogen will be exhausted with the waste gas. However, it can be called truly "0" pollution.

The output form of the fuel cell and the input form of the battery is voltage. In the fuel cell, voltage is not a constant value.

In single cell, the expression of the voltage is:

$$V_{cell} = E_{nernst} + V_{act} + V_{ohmic} + V_{conc}$$

(3.9)

It contains Nernst potential (E_{nernst}) and other overvoltage (V), ohmic (V_{ohmic}), activation (V_{act}) and concentration (V_{conc}) [57].

3.3.1 Nernst equation

In electrochemistry, the Nernst (Nernst) equation is used to calculate the balance voltage of the oxidation-reduction reaction on the electrode. Nernst equation has significant when oxide and reduction materials exist at the same time. On the other hand, while oxide=0 or/and reducer=0, Nernst equation will not be applicable.

In electrochemistry, the Nernst equation is an equation that relates the equilibrium reduction potential of a half-cell in an electrochemical cell to the standard electrode potential, temperature, activity, and reaction quotient of the underlying reactions and species used.

$$E_{nernst} = E_0 - \frac{R_{gas}T}{n_{electron}F} ln \frac{a_{red}}{a_{ox}} \leftrightarrow E_{nernst} = E_0 + \frac{R_{gas}T}{n_{electron}F} ln \frac{a_{ox}}{a_{red}}$$

(3.10)

$\boldsymbol{R_{gas}} =$ *the ideal gas constant* $(8.314472\ J \times K^{-1} \times mol^{-1})$

$\boldsymbol{n_{electron}} =$ *the number of electrons involved in the reaction*(mol)

$[\boldsymbol{oxidized}]/[\boldsymbol{reduced}]$ *It represents the concentration of all the substances involved in the electrode reaction ratio of the concentration of the product and the product of the reaction products. And the concentration should be equal to the square of their second coefficient in the electrode reaction*

Rapport-gratuit.com
LE NUMERO 1 MONDIAL DU MÉMOIRES

In the PEMFC, the oxides are H_2 and O_2, the reduction is H_2O.

$$E_{nernst} = N_{fc}[E_0 + \frac{RT}{2F} log(\frac{p_{H_2} p_{O_2}^{0.5}}{a_{red}})]$$

(3.11)

3.3.2 Activation

In electrochemical, "activation" refers to the reversible transition of a molecule into a nearly identical chemical or physical state, with the defining characteristic being that this resultant state exhibits an increased propensity to undergo a specified chemical reaction. Thus, activation is conceptually the opposite of protection, in which the resulting state exhibits a decreased propensity to undergo a certain reaction[58].

The activation potential is the potential difference above the equilibrium value required to produce a current that depends on the activation energy of the red-ox event. While ambiguous, "activation over-potential" often refers exclusively to the activation energy necessary to transfer an electron from an electrode to an anolyte. This sort of over-potential can also be called "electron transfer over-potential".

The energy of activation specifies the amount of free energy the reactants must possess (in addition to their rest energy) in order to initiate their conversion into corresponding products—that is, in order to reach the transition state for the reaction. The energy needed for activation can be quite small, and often it is provided by the natural random thermal fluctuations of the molecules themselves (i.e. without any external sources of energy).

Activation energy pertains to the temperature dependence of leakage current and may be ascribed to carrier generation and transport mechanisms[59]. Semi empirical expression of the activation voltage is given by equation (3.12). In the equation, k1, k2, k3 and k4 are parametric values.

The activation voltage can be expressed as:

$$V_{act} = k_1 + k_2 T + k_3 T\left[ln\left(C_{O_2}^*\right)\right] + k_4 T[ln(i)]$$

$$k_1 = 6.4382e^{-5}\,;\; k_2 = 3.0301\,; k_3 = 0.045671\,;\; k_4 = 0.076233$$

$$C_{O_2}^* = p_{O_2}/(5.08 \times 10^6 \times e^{\frac{-498}{T}})$$

(3.12)

3.3.3 Ohmic over-potential

Ohmic contact can also be called metal semi-contact. In the fuel cell, the proton exchange membrane is contacted with the electrode. A proton exchange membrane or polymer electrolyte membrane (PEM) is a semi-permeable membrane generally made from ionomers and designed to conduct protons while being impermeable to gases such as oxygen or hydrogen[60][61]. This is their essential function when incorporated into a membrane electrode assembly (MEA) of a proton exchange membrane fuel cell or of a proton exchange membrane electrolyser: separation of reactants and transport of protons[61]. While, the membrane is contacted with the electrode which is made by metal, this form of contact will cause the change of internal resistance. The contact place of metal and semiconductor will cause the potential barrier increasing. Thus, it leads the loss of production. This semi-contact is shown in Figure 3-4.

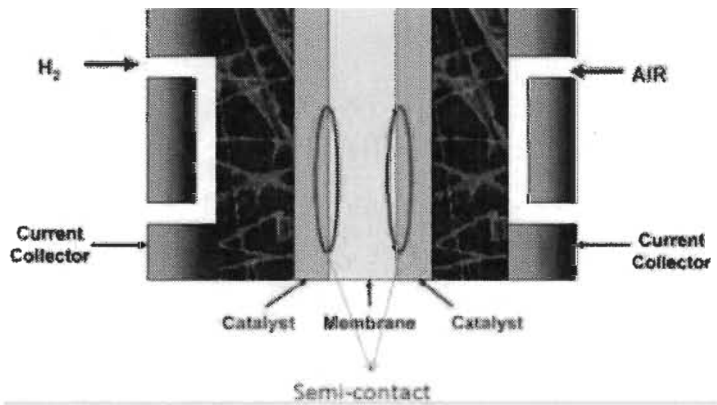

Figure 3-4. Ohmic over-potential caused by semi-contact

The resistance of the ohmic voltage in the fuel cell depends on not only the proton membrane but also the electrode.

$$V_{ohmic} = -i(R_{proton} + R_{electronic}) \quad (3.13)$$

Here, R_{proton} is the resistance of proton, and it can be expressed as:

$$R_{proton} = (r_M \times S_{membrane})/A \quad (3.14)$$

r_M is the resistivity of the proton exchange membrane, $S_{membrane}$ is its thickness and A is the reacting contact area.

Additionally,

$$r_M = 181.6 \times [1 + 0.035\left(\frac{i}{A}\right) + 0.062\left(\frac{T}{303}\right)^2\left(\frac{i}{A}\right)^{2.5}]/k_5$$
$$k_5 = [\lambda - 0.634 - 3\left(\frac{i}{A}\right)]exp[4.18\left(\frac{T-303}{T}\right)] \quad (3.15)$$

While current in the charging circuit is 0, the specific resistivity is (181.6/λ-0.634). λ is the empirical factor of the water content in the proton exchange membrane.

3.3.4 Concentration over-potential

Concentration over-potential spans a variety of phenomena that involve the depletion of charge-carriers at the electrode surface. Bubble over-potential is a specific form of concentration over-potential in which the concentration of charge-carriers is depleted by the formation of a physical bubble. The "diffusion over-potential" can refer to a concentration over-potential created by slow diffusion rates as well as "polarization over-potential", whose over-potential is derived mostly from activation over-potential but whose peak current is limited by diffusion of anolyte[62].

The potential difference is caused by differences in the concentration of charge-carriers between bulk solution and the electrode surface. It occurs when electrochemical reaction is sufficiently rapid to lower the surface concentration of the charge-carriers below that of bulk solution. The rate of reaction is then dependent on the ability of the charge-carriers to reach the electrode surface.

In the fuel cell, the concentration voltage is calculated by the following equation:

$$V_{conc} = \left(\frac{RT}{nF}\right) log(1 - \frac{j}{j_{lim}})$$

(3.16)

$\boldsymbol{j_{lim}} = the\ current\ density\ limit(A/cm^2)$

3.3.4.1 Model of fuel cell

The power of fuel cell is expressed as the follow equation:

$$E_{cell} = E_{r,T,P} - \frac{R_{gas}T}{\alpha_{transfer}F} ln\left(\frac{i_{cell} + i_L}{i_0}\right) - \frac{R_{gas}T}{n_{electron}F} ln\left(\frac{i_L}{i_L - i}\right) - iR_i$$

(3.17)

$\boldsymbol{E_{r,T,P}} = reversible\ voltage\ according\ to\ temperature\ and\ pressure\ (V)$

$\boldsymbol{\alpha_{transfer}} = the\ transfer\ coefficient\ (n/a)$

$\boldsymbol{i_{cell}} = the\ current\ density\ of\ the\ cell\ (A/cm^2)$

$\boldsymbol{i_L} = the\ loss\ of\ current\ (A/cm^2)$

$\boldsymbol{i_0} = the\ exchange\ current\ reference\ (A/cm^2)$

The relationship between the output of voltage and the charge current is shown in Figure 3-5:

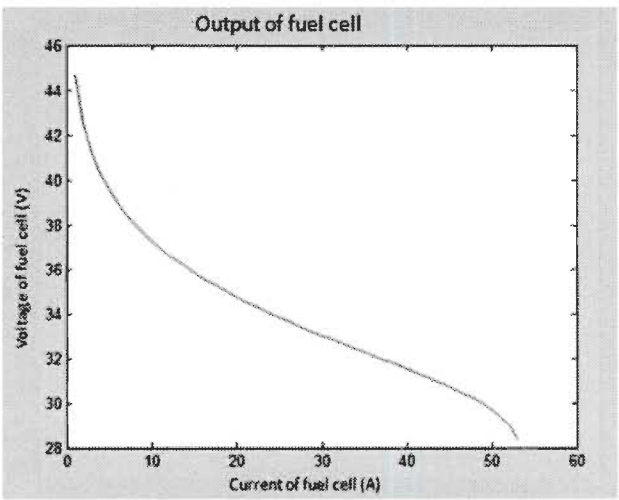

Figure 3-5.Relationship of current and voltage of PEMFC

This model of PEMFC shows the fast response to charge in load. In case of vehicle application transient, load dynamics are faster than the transients in stationary application. When operating, the power demand changes with a high frequency. Therefore, the batteries should deal with fast load transients. It is assumed that this batteries pack is sufficient to give an acceptable response to transient load[57].

Through this graph, it can be found that the voltage is inversely proportional to the current. In the test, the maximum voltage is 44.5V (rated 48V) and the maximum current is 52A (rated 52A). This relationship is caused by the fixed output power (2.5kW).

3.4 Hydrogen consumption

The hydrogen consumption is affected by two elements, the fuel cell series and the output current[63]. The efficiency is constant as its factory setting (no variable in the experiment). Thus, in the simulation, the two variable parameters which can be controlled are the number of fuel cells and the current. Hydrogen consumption can be calculated by:

$$Con_{H_2} = \frac{I_{ch} \times N_{fc}}{2F} \times \eta \times t \tag{3.18}$$

By 137000s simulation, the hydrogen consumption situation is shown in Figure 3-6:

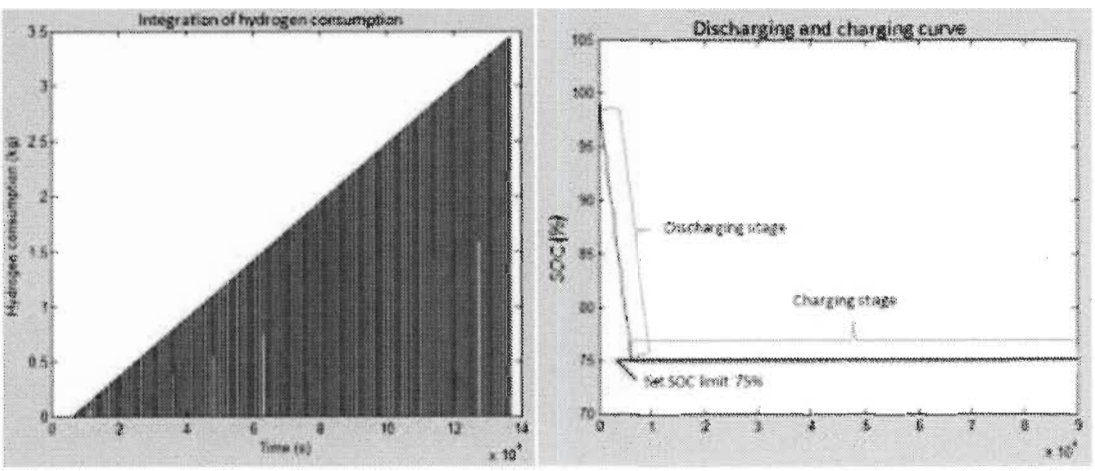

Figure 3-6. a: Integration of the hydrogen consumption; b: The process of discharging and charging (reflected by SOC)

It is clear that the total consumption of the hydrogen is composed by the integration of

each charging cycles. The blank part is the period when the vehicle uses the battery power only without the battery being charged. Therefore, in that period of time, there is no hydrogen consumption. Figure b is synchronous response to figure a. Here, the level limit to start charging is set at 75%. (The reason why choose 75% charging level is that starting charge battery at this level will make the total consumption minimally. The optimization will be presented in Chapter 4.) On the other hand, it shows that the fuel cell in the Nemo is not able to charge the battery to the maximum level but to retard the decreasing rate of the SOC when the vehicle is running. In order to extend fuel cell's life, the topping charge and float charge stage should be finished by the grid, while the vehicle is stop.

3.5 Battery state

SOC (state of charge) is the most important value when monitoring the battery[57]. In Figure 3-7, the battery with 100% (normally 95%) SOC support the vehicle operation for 10 hour at output power level 2.5kW.

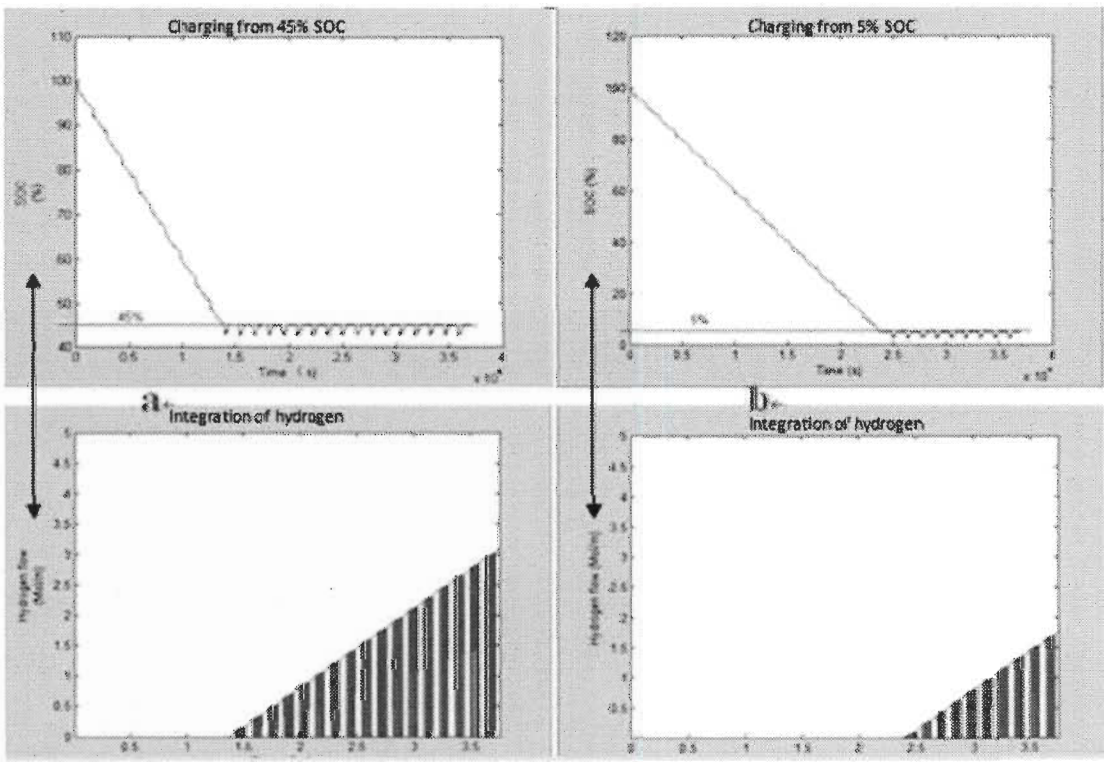

Figure 3-7.Battery SOC of discharge-charge & hydrogen consumption, a: Discharge and switch on fuel cell at 5% (SOC); b: Charge from 45%-95% (SOC)

From the figure, it can be found that the charging curve fluctuate below the set limit of SOC. This phenomenon illustrate that the function of the fuel cell is to reduce the decreasing speed of SOC. Charging the battery to the full state is not available because of the output power is not high enough. However, the increasing rate of hydrogen consumption in "a" is higher than "b". Thus, the preliminary conclusion that can be obtained is switching on the fuel cell at a lower SOC level can reduce the hydrogen consumption. While starting the fuel cell at a high SOC level, more hydrogen will be used.

3.5.1 Power transferring among fuel cell, battery and motor

Mentioned in equation (2.1), the power of mechanical is the sum of fuel cell power and battery power.

Here,

$$P_{fuel\ cell} = V_{fuel\ cell} \times I_{fuel\ cell} \tag{3.19}$$

While the level of remaining power is higher than the limit of SOC, the fuel cell will not charge the battery. During this time the status of fuel cell is off. Therefore, the relationship becomes:

$$P_{output} = P_{toruqe} = P_{battery} \tag{3.20}$$

With the of power level decreasing in the battery, the fuel cell will be switched on while the battery needs to be charged (lower than the set SOC limit). Since then, the current in the battery is divided into two parts. One is the output of the battery and another is the charging power supported the fuel cell.

While the battery is being charged,

$$P_{battery} = -(V_{fuel\ cell} \times I_{charge})$$

(3.21)

Else, the vehicle is operating,

$$P_{battery} = V_{battery} \times I_{discharge}$$

(3.22)

3.5.2 Charging-discharging circuit

While the vehicle is running and the fuel cell is switched on to charge the battery, the power of fuel cell supports the motor indirectly through the battery. While the supported power from fuel cell is larger than the required mechanical power, the remaining power will be stored in the battery and the level of SOC will be increased. If the supported power from fuel cell is smaller than the required mechanical power, all of the electric power will be used to drive the motor and the short part of energy will be complemented by the battery. At the same time, the SOC level decreases continuously until the level drop to 0% or all hydrogen is used.

While, $P_{fuel\ cell} > P_{torque}$

$$E_{torque} = E_{FC} - E_{battery} \times SOC = P_{torque} \times t$$

(3.23)

Here,

$$P_{torque} = I_{ch} \times V_{FC} - I_{dis} \times V_{battery}$$

(3.24)

Rapport-Gratuit.com

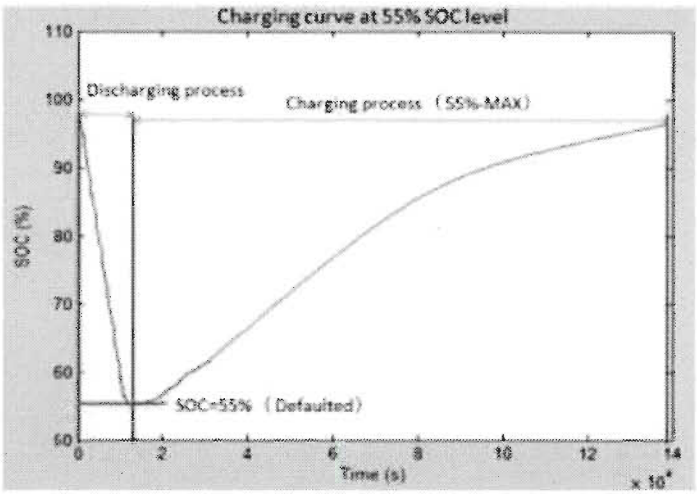

Figure 3-8. SOC level when the power of fuel cell is larger the required power of mechanical

Figure 3-8 is the curve of the discharging and charging process. In this process, the charging level is set at 55%. Obviously, in the charging process, a part of energy is shared by the motor.

Or, $P_{\text{fuel cell}} < P_{\text{torque}}$

$$E_{torque} = E_{FC} + E_{battery} \times SOC = P_{torque} \times t \tag{3.25}$$

$$P_{torque} = I_{ch} \times V_{FC} + I_{dis} \times V_{battery} \tag{3.26}$$

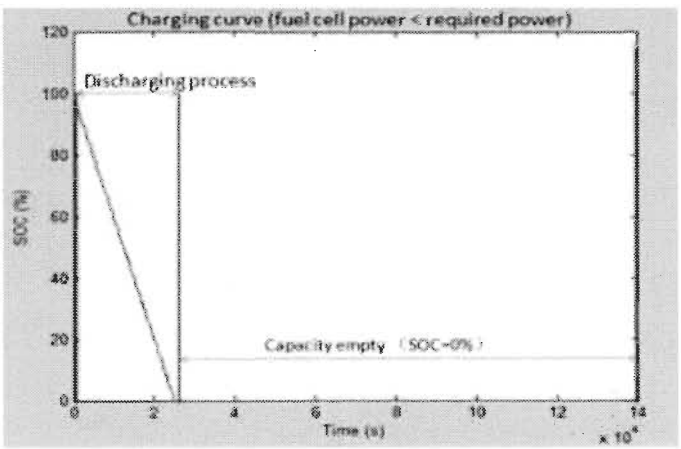

Figure 3-9. Battery status in the operating process without charging

This curve (Figure 3-9) shows the battery discharging process without the power supported from fuel cell. The SOC decreases continuously until the SOC=0 (electric capacity = 0) and the motor will stop.

3.6 Chapter summary

Models of the three parts are given in this chapter. Dynamic model, fuel cell model and battery model built up the integrated simulator. Here, the variable parameter is the limit of SOC. The variations of hydrogen consumption in different charging situation can be obtained through adjusting the value of SOC. This is the preparation for integrating with the battery loss cost which is to optimize the total operating cost.

Rapport-gratuit.com
LE NUMERO 1 MONDIAL DU MÉMOIRES

Chapter 4 - Optimization of the Nemo truck

By analysis the curve of the total consumption, the economy optimization can be achieved. In order to get the further optimization, a new charging method is added in the charging circuit. With the increasing of the charging efficiency, the hydrogen consumption will be reduced about 17%.

4.1 Hydrogen and battery loss consumption

In the operation of the hybrid electric vehicles, the consumption is assumed by hydrogen and the battery jointly. Specifically, charging battery consumes hydrogen and discharging results the reducing of battery's life. Therefore, the operation consumption is the sum of hydrogen cost and the battery loss cost.

The following equation is the economy model of the totally Nemo operation consumption.

$$Cost_{Total} = Cost_{hydrogen} + Cost_{battery} + Cost_{fuel\ cell} \tag{4.1}$$

The charging cycles depends on the specific conditions of the vehicles driving. Table 4-1 is the test data of the Nemo. The length of time of the test is 137000 second and the battery charging cycle is 55. At the same driving condition, the variable parameter of the test is time of start charging at different SOC level.

In the operating process, the cost of hydrogen is expressed by equation (4.2):

$$Cost_{Hydrogen} = (\frac{I_{ch} \times n_f}{2F} \times \eta) \times (t_1 - t_0) \times A_{cost}$$

(4.2)

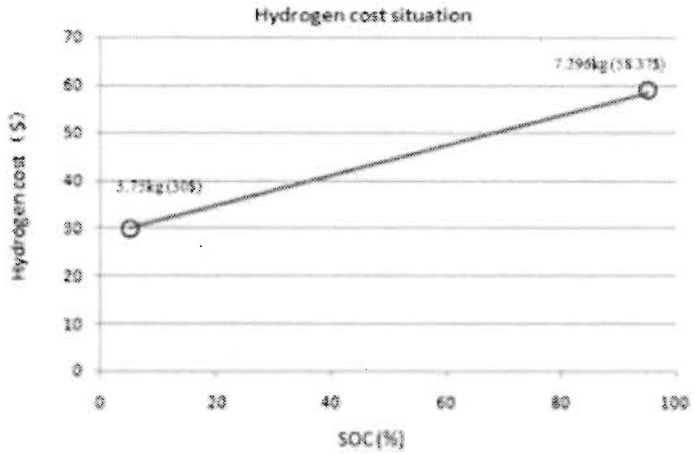

Figure 4-1. Cost of hydrogen consumption

With the increasing of SOC, the consumption of hydrogen increases. The minimum cost is 3.75kg (30$) and the maximum cost is 7.296kg (58.37$).

$$Cost_{battery} = \frac{P_B}{L_B} \times C_{Ch} \times n_B$$

(4.3)

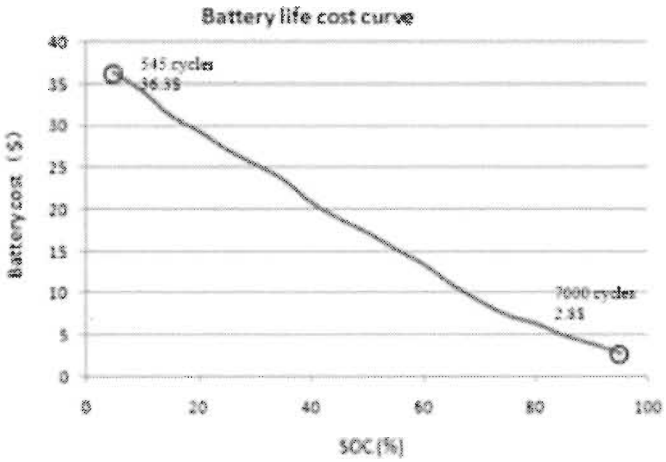

Figure 4-2. Cost of battery life loss

Mentioned in chapter.2, Figure 2-9 is the life curve of the lead-acid battery. The DOD and

the charge cycles are proportional to each other inversely. That means the more capacity be used in each charge cycle, the shorter the battery life will be.

Synchronously, the trend of the battery cost is opposite to the cost of hydrogen. The minimum cost is 2.8$ and the maximum cost is 36.3$.

4.2 Starting time optimization of the fuel cell

Table 4-1 is the comprehensive comparison of the running costs. From the data, it can be easily found that starting fuel cell in the interval of 70-75% SOC it is the minimize cost of the operating. Therefore, this balance time is the best period to starting fuel cell to charge the battery. According to the economic optimization, the operating cost can be given by expression (2.3),

$$Cost_{Total} = (\frac{I_{ch} \times n_f}{2F} \times \eta) \times (t_1 - t_0) \times A_{cost} + \frac{P_B}{L_B} \times C_{Ch} \times n_B + \frac{Power_f \times Price_f}{Life_f} \times (t_1 - t_0) \quad (4.4)$$

Summing the three parts, the total consumption is presented in Figure 4-3:

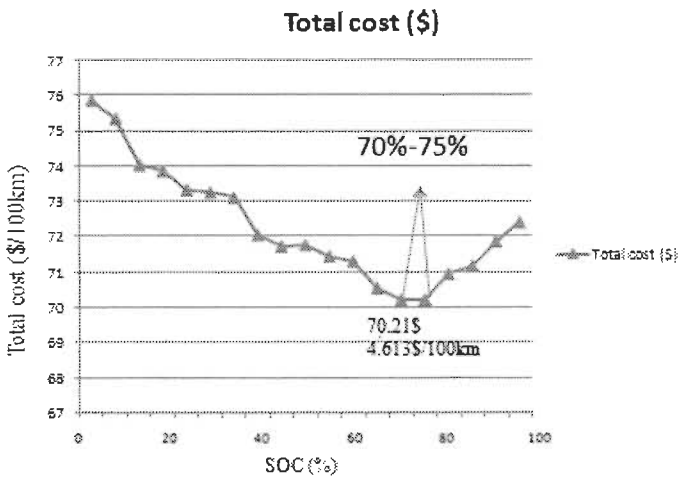

Figure 4-3.Cost curve of battery loss + hydrogen consumption + fuel cell aging

Table 4-1. Data of simulation (137000 second; 100 UDDS loops)

SOC (%)	Available charge cycles (Battery)	Hydrogen (kg)	Hydrogen cost ($)	Battery cost ($)	Fuel cell cost ($)	Total cost ($)	Total cost ($/100km)
5	545	3.75	30	36.330	9.5	75.830	4.9822
10	580	3.947	31.576	34.137	9.59	75.307	4.9479
15	635	4.144	33.152	31.181	9.69	74.021	4.8634
20	675	4.341	34.728	29.333	9.78	73.843	4.8517
25	730	4.538	36.304	27.123	9.88	73.303	4.8162
30	780	4.735	37.88	25.384	9.97	73.234	4.8117
35	840	4.932	39.456	23.571	10.06	73.091	4.8023
40	950	5.129	41.032	20.842	10.16	72.032	4.7327
45	1050	5.326	42.608	18.857	10.25	71.717	4.7120
50	1150	5.523	44.184	17.217	10.35	71.747	4.7140
55	1300	5.72	45.76	15.230	10.44	71.430	4.6932
60	1475	5.917	47.336	13.423	10.53	71.293	4.6842
65	1800	6.114	48.912	11	10.63	70.54	4.6346
70	2300	6.311	50.488	9	10.72	***70.21***	***4.6130***
75	2700	6.508	52.064	7.333	10.82	***70.213***	***4.6132***
80	3100	6.705	53.64	6.387	10.91	70.937	4.6607
85	4000	6.902	55.216	4.95	11.00	71.17	4.6760
90	5000	7.099	56.792	3.96	11.10	71.85	4.7207
95	7000	7.296	58.368	2.828	11.19	72.388	4.7561

From the table, it can be found that the curve of the operating cost is a reverse parabola because the amount of hydrogen is proportional to the battery life. In other words, the more hydrogen costs, the longer the battery life will be. Therefore, the lowest sum cost of hydrogen and battery is the best starting time for the fuel cell.

In Figure 4-3, summing up the three parts of cost, the lowest total consumption can be found at 70%-75% SOC level. Converting into the cost of per 100km, the optimized price is 4.613$/100km Therefore, the best time for switching on the fuel cell is the SOC level 70%-75%.

4.3 Optimization of the circuit

Therefore, automatically control the switch of fuel cell becomes very important in the driving process. In order to implement this method, the optimized control circuit is given and the new control circuit is shown in Figure 4-4.

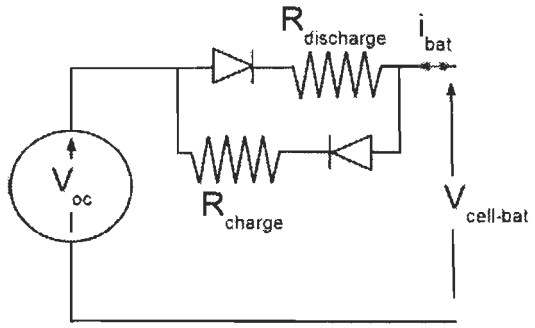

Figure 4-4. Present charging-discharging circuit

4.3.1 Monitoring and controlling of the SOC

As the function of the petrol gauge in the internal combustion engine vehicles, the SOC gauge is used to measure the remaining electric capacity in the battery. With the help of the gauge, the driver will be able know the real time SOC situation. Thus, the time when to start the fuel cell for generating and charging the battery can be grasped accurately. Additionally, the driver can optimize the consumption easily.

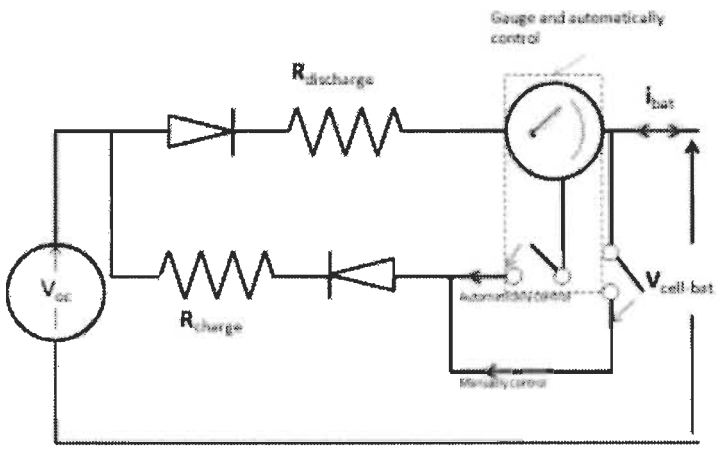

Figure 4-5. Optimized automatically-manually control of the charging circuit

In the charging circuit (Figure 4-5), two control systems are set. Automatically control

and manually control methods both exist in the circuit. While the driver forgets or cannot (leave the vehicle without turning off) to switch on the fuel cell, the automatically control system can start the fuel cell at the previously set SOC level. While the driver wants to start the fuel cell (the SOC level is still higher than the previously set level), the fuel cell can be switched on manually also. So the optimized circuit reduces the difficulties of operating effectively.

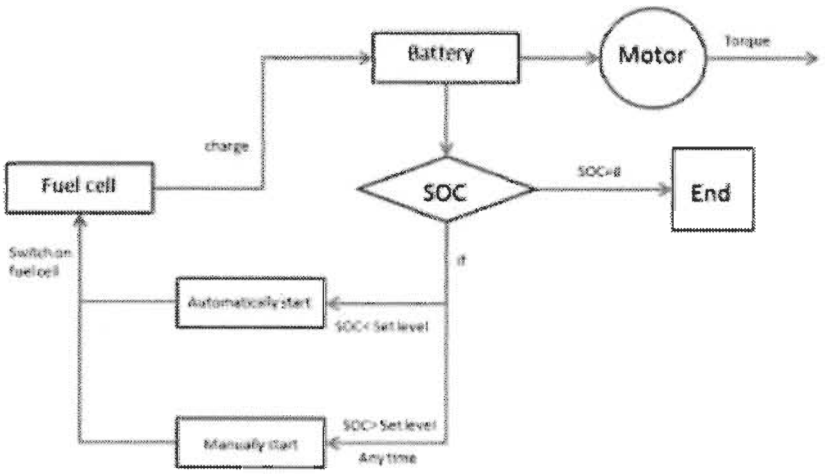

Figure 4-6. Flowchart of automatically-manually charging circuit

The flowchart of the automatically-manually charging model is shown in Figure 4-6. When the SOC is higher than the set level (optimized level), the fuel cell can be started manually anytime. Else, if the SOC is lower than the set level and the fuel cell is not started at this time, fuel cell will be started automatically. The reason to modify the charging control system is to avoid the increasing of DOD which is caused by human negligence.

4.4 Further modified circuit

As Figure 4-7 shows, the volatility of the SOC level is about 2.2% and this phenomenon will cause following two problems:

The first problem is the deepening of the depth of discharge. The charging level is set at 75% (DOD=25%) according to the optimized consumption. However, the actual DOD is

27.5%. This means the life of battery will be shortened (≈ 300 cycles).

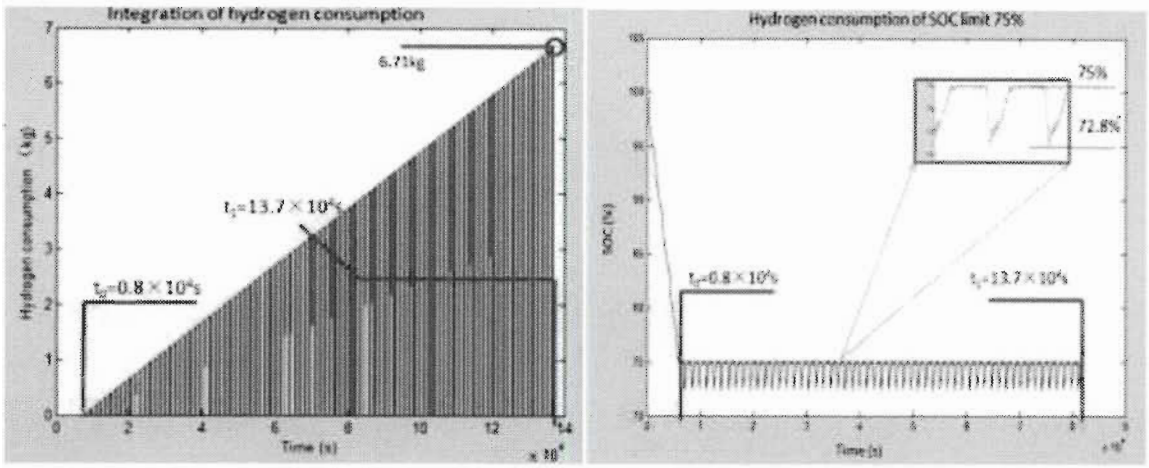

Figure 4-7. Hydrogen consumption and charging curve of SOC limit 75%

Secondly, the hydrogen consumption is increased because of the increasing of the charging rate in each cycle. As shown in Figure 4-7, the hydrogen totally be consumed is 6.71kg (0.44 kg/100km).

4.5 New charging circuit with variable resistor

To solve the problem of the charging wave volatility, the most effective method is reducing the resistance of the charging circuit. In the safe range according to the maximum current of output of the fuel cell and the load of the battery, the input of the charging current would be increased from 20A to 40A.

To increase the current in a circuit, there are two methods. One is increasing the input voltage and another is reducing the resistance. However, the output voltage of the fuel cell is limited with the certain series number. So the charging circuit cannot obtain an increased input voltage. Thus, the only method available is reducing the resistance in the charging circuit[66].

Figure 4-8 shows the change of the charging circuit. A smaller resistor is installed parallel in the charging circuit. Then, the resistance of the circuit becomes variable and the higher efficiency charging can be achieved.

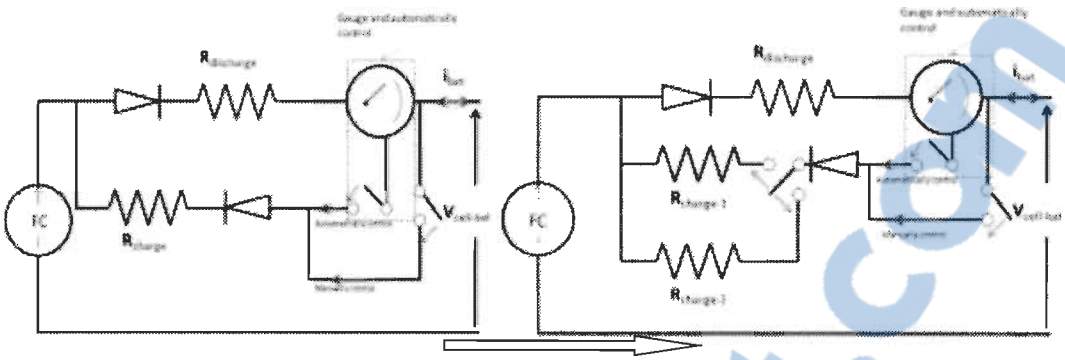

Figure 4-8.The charging circuit with variable resistance installed

With the optimization of the charging circuit, the charging resistance is modified from the constant resistance the variable resistance.

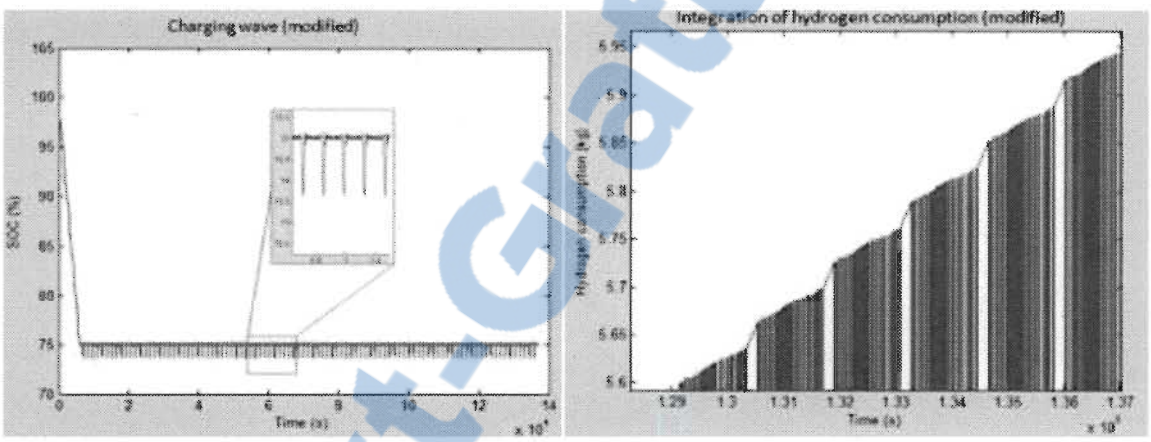

Figure 4-9. Charging situation after increase the charging current

The result of the changes is shown in Figure 4-9, the volatility of charging wave decreases from 2.5% to 1.4%. This means the DOD is reduced 1.1%. It can save the battery life about 200 charging cycles (increase from 2500 to 2700 cycles). This decreasing of DOD is caused by the rising of the charging current. The rising of current will improve the charging efficiency. Therefore, the charging response became faster and the SOC will not go downward too much. Additionally, the hydrogen consumption (137000 seconds) decreased to 5.94kg (with 0.56kg saving, ≈9%). According to the result of simulation, increasing the current is a method which can reduce the cost of the operation effectively. Therefore, the difference between original and modified consumption is affects by the difference of charging time and the battery life which can be calculated by the deeper

Rapport-Gratuit.com

modified equation as follow:

$$\Delta_{cost} = \left(\frac{I_{ch} \times n_f}{2F} \times \eta \times A_{cost}\right) \times (t_1 - t_0) + \left(\frac{P_B}{L_B} - \frac{P_B}{L'_B}\right) \times C_{ch} \times n_B \quad (4.6)$$

Additionally, the DOD is reduced to 25.3% (before modified is 26.5%). At this DOD level, the lead-acid battery life is 2700 cycles (before modified is 2500). Thus, the battery life is extended by 200 charging cycles.

$$L_B = 2500$$

$$L'_B = 2700$$

Table 4-2. Comprehensive data analysis

SOC (%)	Available charge cycles (Battery)	Hydrogen (original) (kg/100km)	Cost (original) ($/100km)	Hydrogen (optimized) (kg/100km)	Cost (optimized) ($/100km)
5	545	0.246386	4.982278	0.246386	4.765277
10	580	0.25933	4.947959	0.253876	4.700426
15	635	0.272273	4.86341	0.261367	4.589912
20	675	0.285217	4.85173	0.268857	4.545642
25	730	0.29816	4.816248	0.276347	4.479733
30	780	0.311104	4.811736	0.283837	4.441979
35	840	0.324047	4.802328	0.291327	4.399775
40	950	0.336991	4.732727	0.298817	4.30285
45	1050	0.349934	4.712033	0.306307	4.250385
50	1150	0.362878	4.71402	0.313798	4.218539
55	1300	0.375821	4.693217	0.321288	4.165976
60	1475	0.388765	4.684213	0.328778	4.124139
65	1800	0.401708	4.634691	0.336268	4.045466
70	2300	0.414652	4.613009	0.343758	4.031438
75	2700	0.427595	4.613228	0.351248	4.156084
80	3100	0.440539	4.660782	0.358739	4.22458
85	4000	0.453482	4.676084	0.366229	4.293075
90	5000	0.466426	4.720762	0.373719	4.36157
95	7000	0.479369	4.756148	0.381209	4.430066

In the table, it can be found that the lowest cost interval is in the level of SOC 65%-70%.

Before the optimization of the charging circuit, the minimal cost is in the interval of 70%-75%. This change is caused by the decreasing of the hydrogen consumption which is modified by the improvement of charging efficiency.

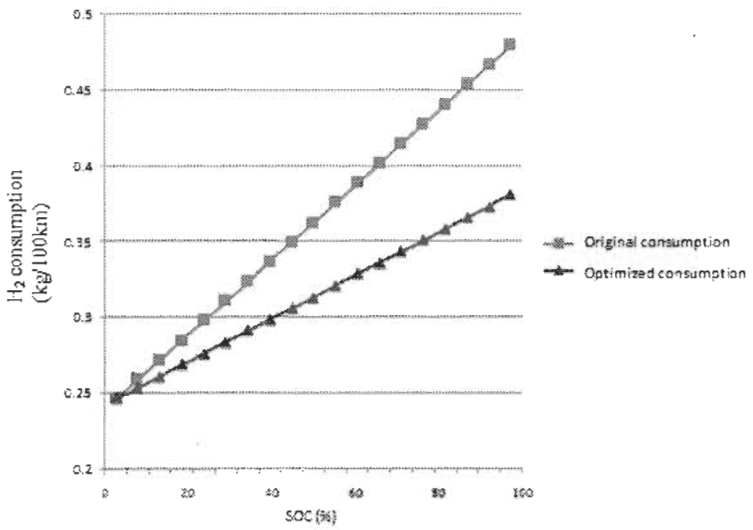

Figure 4-10. Hydrogen consumptions comparison of original and optimized models

Focus on hydrogen consumption independently, the consumption increases with the decreasing of DOD. That means the start the fuel cell later; the more hydrogen will be saved. However, the cost of battery loss affects the total cost corporately. The comparison curves of the total cost is shown in Figure 4-11

Rapport-gratuit.com
LE NUMERO 1 MONDIAL DU MÉMOIRES

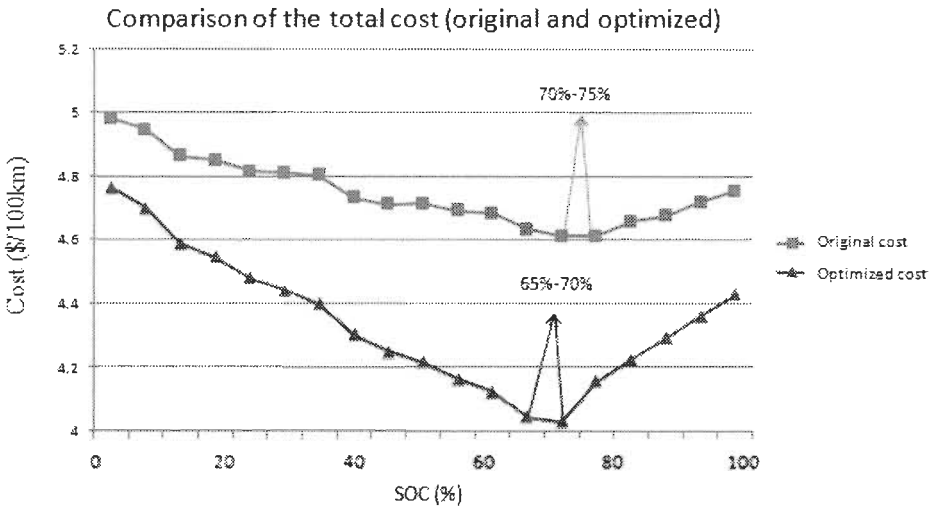

Figure 4-11. Comparison of the total cost

Comparing the original data and the optimized data, the hydrogen consumption is saved about 0.08kg/100km (about 17.6%) and the total cost per 100/km is saved about 0.57$.

4.6 Chapter summary

Firstly, the best starting time of the fuel cell is given by the economic optimization. The result is that starting the fuel cell at 70%-75% SOC level, the total operating cost will be the minimal.

Secondly, with the participation of the automatically control of the fuel cell switching, the unnecessary increasing of DOD can be avoided.

Finally, the variable charging resistance is added in the charging circuit. It can help adjust the input current of the battery. It not only shortens the charging process, but also decreases the DOD which can increase the charging cycles of battery. Additionally, the consumption of hydrogen is reduced because of the increasing of the charging efficiency.

Chapter 5 - Conclusions and discussion

5.1 Discussion of the results observed

The objective of this thesis is the economy optimization of the Nemo truck. For minimizing the operating costs of Nemo, the work is approached from three part : the fuel cell starting time optimization, the automatically charging system and the optimization of the charging circuit.

Through analyzing the overall operating consumption of Nemo, the most appropriate time for switching on the fuel cell can be obtain. Therefore, by controlling the switching time of the fuel cell, the total cost of the Nemo can be artificially reduced.

Secondly, with the participation of the automatically charging system, the fault tolerance is improved. The unnecessary deepening of the battery can be avoided. Thus, the battery life can be controlled in the range of normal aging.

Finally, the charging circuit is modified by the variable charging resistor being added. The result of simulation shows two advantages. The first one is the decrease of the DOD (depth of discharge) which can extend the battery life obviously. The second one is the reducing of the hydrogen of consumption which is caused by the improvement of the charging efficiency.

Following the above optimizations, a brief appraisal about the pros and cons is necessary to be presented here.

Although the controlling of the fuel cell switching time reduced the operating cost effectively, there are still many factors that affect on the operating status of Nemo. With the accumulation of the tests time, more and more problems will be faced. The preset optimization will be improved through the analysis of more conditions in the future work.

The modified charging circuit has a significant impact on the operating costs of Nemo.

Theoretically, with the decrease of the charging resistance, the charging efficiency could be increased unlimited. However, the optimization is nonlinear because it is limited by the output of fuel cell. The further optimization maybe damages the fuel cell. Additionally, the overheating in the charging process is another factor which cannot be ignored. Therefore, if the further optimization is hoped to be achieved, these problems should be solved[25].

5.2 Prospects and future work

All these work for the optimization of the Nemo is to make it to be able to commercialize as soon as possible. Nemo truck has many advantages, however, the potential of developing and optimization still exist. The energy management is the preliminary stage of a vehicle. The future works such as: embedded systems, safety facilities and the exterior designing are following. There are many parts that can be optimized. Here are some examples.

References

[1] Cook Brain, "An Introduction to Fuel Cells and Hydrogen Technology," no. December, 2001.

[2] "Fuel Cell-WIKIPEDIA." [Online]. Available: http://en.wikipedia.org/wiki/Fuel_cell.

[3] J. Lee, Y. Kim, and H. Cha, "A new battery parameter identification considering current, SOC and Peukert's effect for hybrid electric vehicles," *2011 IEEE Energy Convers. Congr. Expo.*, pp. 1489–1494, Sep. 2011.

[4] Paulsmith99, "Fuel Cell Block Diagram," 2010. [Online]. Available: http://en.wikipedia.org/wiki/File:Fuel_Cell_Block_Diagram.svg.

[5] J. W. Ritter, C. F. Schoenbein, and W. R. Grove, "Discovering the principle of the fuel cell at home or in school," pp. 1–8, 2000.

[6] "Comparison of fuel cell types." [Online]. Available: http://en.wikipedia.org/wiki/Fuel_cell.

[7] M. Cifrain, K. Kordesch, A. Lamm, and H. A. Gasteiger, "Hydrogen / oxygen (Air) fuel cells with alkaline electrolytes," vol. 1, pp. 267–280, 2003.

[8] "AFC-FuelCellToday." [Online]. Available: http://www.fuelcelltoday.com/technologies/afc.

[9] A. Verma, "Performance of Alkaline Fuel Cells : A Possible Future Energy System."

[10] M. a. Tanni, M. Arifujjaman, and M. T. Iqbal, "Dynamic Modeling a of Phosphoric Acid Fuel Cell (PAFC) and Its Power Conditioning System," *J. Clean Energy Technol.*, vol. 1, no. 3, pp. 178–183, 2013.

[11] "MCFC-FuelCellToday." [Online]. Available: http://www.fuelcelltoday.com/technologies/mcfc.

[12] S. Mcphail, A. Moreno, R. Bove, and R. Rse, "International Status of Molten Carbonate Fuel Cell (MCFC) Technology," 2009.

[13] "PEMFC-FuelCellToday." [Online]. Available: http://www.fuelcelltoday.com/technologies/pemfc.

[14] F. Barbir, "PEM Fuel Cells," 2005.

[15] S. Litster and G. McLean, "PEM fuel cell electrodes," *J. Power Sources*, vol. 130, no. 1–2, pp. 61–76, May 2004.

[16] "PEM Fuel Cells," *Neutorn Imaging Facility*. [Online]. Available: http://physics.nist.gov/MajResFac/NIF/pemFuelCells.html.

[17] "Proton exchange membrane fuel cell," *Energy.GOV*. [Online]. Available: http://www1.eere.energy.gov/hydrogenandfuelcells/fc_animimation_process.html.

[18] PHYWE Systeme GmbH & Co.KG, *Characteristics and efficiency of PEM fuel cell and PEM electrolyser Set-up and procedure*. pp. 1–12.

[19] S. C. Lee, O. Kwon, and D.-H. Lee, "Fuel cell simulation: Steady-state and dynamic case," *2012 7th Int. Conf. Comput. Sci. Educ.*, no. Iccse, pp. 974–979, Jul. 2012.

[20] J.-H. Wee, "Applications of proton exchange membrane fuel cell systems," *Renew. Sustain. Energy Rev.*, vol. 11, no. 8, pp. 1720–1738, Oct. 2007.

[21] E. C. Nantes and N. Bp, "Fuel Cell Technology and Application," 2007.

[22] Z. X. Jing, W. Y. Shao, X. Y. He, Q. H. Wu, S. Huang, M. Liu, and W. H. Wu, "Research on unit commitment in power system with electric vehicles classification," *2013 IEEE Power Energy Soc. Gen. Meet.*, pp. 1–5, Jul. 2013.

[23] "2012 Mitsubishi i Electric Car: X-Ray Cutaway Shows Layout," *Green Car Reports*. [Online]. Available: http://www.greencarreports.com/news/1063854_2012-mitsubishi-i-electric-car-x-ray-cutaway-shows-layout.

[24] Y. . Chau, K.T., Wong, "Overview of power management in hybrid electric vehicles," *Energy Convers. Manag.*, vol. 43, pp. 1953–1968, 2002.

[25] F. Martel, "Modelisation D'un Vehicule Electrique Hybride et de la Degradation de ses Batteries Inculant sa Validation Experimentale," Université du Québec à Trois-Rivières, 2011.

[26] R. N. T. Dincer Mehmet B., Mehmet Ali C., "Development of Control Strategy Based on Fuzzy Logic Control for a Parallel Hybrid Vehicle," *Tubitak Marmara Research Center,Energy Institute, Gebze, Kocaeli, Turkey*.

[27] H. Uwe Sauer, D., Wenzl, "Comparison of different approaches for lifetime prediction of electrochemical systems—Using lead-acid batteries as example," *J. Power Sources*, vol. 176, pp. 534–546, 2008.

[28] "What is a Hybrid Electric Vehicle?," *global-greenhouse-warming*. [Online]. Available: http://www.global-greenhouse-warming.com/hybrid-electric-vehicle.html.

[29] "Fuel cell car." [Online]. Available: http://commons.wikimedia.org/wiki/File:Fuelcell.jpg.

[30] N. Xue, W. Du, T. A. Greszler, W. Shyy, and J. R. R. A. Martins, "Design of a Lithium-ion Battery Pack for PHEV Using a Hybrid Optimization Method," pp. 1–23, 2013.

[31] S. Kelouwani, K. Agbossou, Y. Dubé, and L. Boulon, "Fuel cell Plug-in Hybrid Electric Vehicle anticipatory and real-time blended-mode energy management for battery life preservation," *J. Power Sources*, vol. 221, pp. 406–418, Jan. 2013.

[32] C. C. Chan, "The state of the art of electric and hybrid vehicles," *Proc. IEEE*, vol. 90, no. 2, pp. 247–275, 2002.

[33] "Urban Truck." [Online]. Available: http://www.nev-nemo.com/Site/Home_Nemo.html.

[34] "US 8VGCHC XC2." [Online]. Available: http://usbattery.com/products/8-volt-batteries/us-8vgchc-xc2/.

[35] U. S. Xc, "Golf car and utility vehicles," vol. 92879, no. 800, 1895.

[36] "Axane PEMFC." [Online]. Available: http://www.fuelcellmarkets.com/fuel_cell_markets/member_view.aspx?articleid=2595&subsite=1&language=1.

[37] "Axane PEM fuel cell." [Online]. Available: http://www.horizonhydrogeneenergie.com/technologie-axane.html.

[38] J. Spendelow and J. Marcinkoski, "DOE Fuel Cell Technologies Office Record 14012: Fuel Cell System Cost - 2013," pp. 1–8, 2014.

[39] L. Boulon, K. Agbossou, D. Hissel, A. Hernandez, A. Bouscayrol, P. Sicard, and M. Péra, "Energy Management of a Fuel Cell System : Influence of the Air Supply Control on the Water Issues," pp. 161–166, 2010.

[40] S. Wasterlain, D. Candusso, D. Hissel, F. Harel, P. Bergman, P. Menard, and M. Anwar, "Study of temperature, air dew point temperature and reactant flow effects on proton exchange membrane fuel cell performances using electrochemical spectroscopy and voltammetry techniques," *J. Power Sources*, vol. 195, no. 4, pp. 984–993, Feb. 2010.

[41] F. Martel, Y. Dubé, L. Boulon, and K. Agbossou, "Hybrid electric vehicle power management strategy including battery lifecycle and degradation model," 2011.

[42] L. Wang, "A parametric study of PEM fuel cell performances," *Int. J. Hydrogen Energy*, vol. 28, no. 11, pp. 1263–1272, Nov. 2003.

[43] V.-T. Liu and K.-C. Tseng, "Power converter design for a fuel cell electric vehicle," *2010 5th IEEE Conf. Ind. Electron. Appl.*, pp. 510–515, Jun. 2010.

[44] U. Nations, *Recommendations on the Transport of Dangerous Goods: Manual of Tests and Criteria*. United Nations Publications, 2009, p. 394.

[45] "Battery Life (and Death)," *Electropaedia*, 2005. [Online]. Available: http://www.mpoweruk.com/life.htm.

[46] "Relationship of DOD and battery life," *Heatspring magazine*.

[47] CivicSolar, "How does Depth of Discharge factor into Grid Connected battery systems?"

[48] "Lead-Acid battery charging status." [Online]. Available: http://batteryuniversity.com/learn/article/charging_the_lead_acid_battery.

[49] K. Maalej, S. Kelouwani, K. Agbossou, and Y. Dubé, "Enhanced fuel cell hybrid electric vehicle power sharing method based on fuel cost and mass estimation," *J. Power Sources*, vol. 248, pp. 668–678, Feb. 2014.

[50] H. Ikeda, S. Minami, S. J. Hou, Y. Onishi, and A. Kozawa, "Nobel High Current Pulse Charging Method for Prolongation of Lead-acid Batteries," pp. 2–8, 2004.

[51] G. Yifeng and Z. Chengning, "Study on the fast charging method of lead-acid battery with negative pulse discharge," *2011 4th Int. Conf. Power Electron. Syst. Appl.*, pp. 1–4, Jun. 2011.

[52] T. K. Cheung, K. W. E. Cheng, H. L. Chan, Y. L. Ho, H. S. Chung, and K. P. Tai, "Maintenance techniques for rechargeable battery using pulse charging," *2006 2nd Int. Conf. Power Electron. Syst. Appl.*, pp. 205–208, Nov. 2006.

[53] W. W. M.Bhatt, W.G.Hurley, "A new approach to intermittent charging of valve-regulated lead-acid batteries in standby applications," in *Power Electronics Specialist Conference, 2003. PESC '03. 2003 IEEE 34th Annual*, 2003, vol. 2.

[54] K. a. Buckle and J. W. Luce, "Battery vehicle charger design eliminates harmonic current generation," *Proc. SOUTHEASTCON '96*, pp. 561–564.

[55] J. R. Diego Feroldi, Maria Serra, "Energy Management Strategies based on Efficiency Map for Fuel Cell Hybrid Vehiclese."

[56] "UDDS-WIKI." [Online]. Available: http://en.wikipedia.org/wiki/UDDS.

[57] K. Ettihir, L. Boulon, K. Agbossou, S. Kelouwani, and M. Hammoudi, "Design of an energy management strategy for PEM Fuel Cell Vehicles," *2012 IEEE Int. Symp. Ind. Electron.*, pp. 1714–1719, May 2012.

[58] E. M. A. N. Sssr, M. Inst, and N. Sinteza, "On activation energy of chemical reactions," p. 20017908, 1988.

[59] L. C. Burton and S. Member, "Voltage Dependence of Activation Energy for Multilayer Ceramic Capacitors," vol. C, no. 4, pp. 517–524, 1986.

[60] L. B. Johnson, "Alternative Electrochemical Systems for Ozonation of Water Hydrogen gas , ozone gas , and ozonated water can be delivered under pressure . Interferometer for Measuring Displacement to Within 20 pm," no. July, pp. 24–25, 2003.

[61] "Proton exchange membrane." [Online]. Available: http://en.wikipedia.org/wiki/Proton_exchange_membrane.

Rapport-Gratuit.com

[62] G. D. . E. B. Short, "Concentration Overpotentials on Antimony Electrodes in Differential Electrolytic Potentiometry," *Anal. Chem.*, vol. 37, pp. 962–967.

[63] J. Lavminie, A. Dicks, and J. Wiley, "Fuel cell systems explained," no. October, p. 308, 2000.

[64] J. J. A. Wilkinson and B. E. Hons, "A new pulse charging methodology for lead acid batteries," vol. 25, no. 1, pp. 1–16, 1998.

[65] Z. Yue, Z. Lisheng, C. Lin, and X. Chuanxiang, "Dynamic Polarization Modeling of Suspended Cells Under AC field," pp. 293–296.

[66] J. Yan, G. Xu, H. Qian, and Y. Xu, "Battery Fast Charging Strategy Based on Model Predictive Control," *2010 IEEE 72nd Veh. Technol. Conf. - Fall*, pp. 1–8, Sep. 2010.

Chapter 6 - Appendix A- Résumé du travail de recherche

6.1 Introduction

Une pile à combustible agit comme convertisseur d'énergie électrique et d'énergie chimique. Cette réaction électro-chimique entre l'hydrogène et l'oxygène produit de l'électricité, de l'eau et de la chaleur. Pile à combustible à membrane électrolyte polymère (PEMFC, ou pile PEM) est une une pile à combustible de carburant basse température (environ 70°C) [19]. En ajustant les paramètres de fonctionnement tels que la température, le temps de commutation; les meilleures conditions de travail se trouvent qui est appelé optimisation. L'efficacité et la puissance des PEMFC sont principalement affectées par la variation des paramètres d'exploitation [18]. Par conséquent, ce travail présente la méthode de gestion efficace et l'optimisation de la consommation. En utilisant ces procédés, l'utilisation du combustible et de l'efficacité économique seront améliorées.

6.1.1 Travaux existants

Nemo est un véhicule de la batterie qui est modifié pour être un véhicule électrique hybride IRH-UQTR. Pour améliorer son endurance, économie énergie et l'environnement de protection, une pile à combustible à membrane échangeuse de protons de 2.5 kW et un générateur de moteur à combustion interne 5kW sont tous deux installés. L'objectif de l'optimisation est de se débarrasser du combustible fossile progressivement sous la prémisse de sa stabilité de travail. Pour améliorer les performances du véhicule, le rendement énergétique est le facteur le plus important. Non seulement dans le système de pile à combustible, mais aussi dans le système de batterie, le contrôle de la gestion de l'énergie est la méthode efficace pour augmenter le rendement du carburant.

Rapport-gratuit.com
LE NUMERO 1 MONDIAL DU MÉMOIRES

6.1.1.1 Gestion de l'énergie de la pile à combustible

L'objectif de cette optimisation est obtenir une alimentation en air à partir d'une pompe de compresseur ou de l'air. Parce que, dans une pile à combustible, la pression de l'air est très importante [41]. Elle affecte la qualité de la conversion d'énergie et d'efficacité dans l'empilement de piles à combustible. Le problème de la gestion de l'eau est souvent négligée. L'alimentation en gaz a un impact important. Par conséquent, la précision du contrôle de gestion de l'énergie est fortement nécessaire.

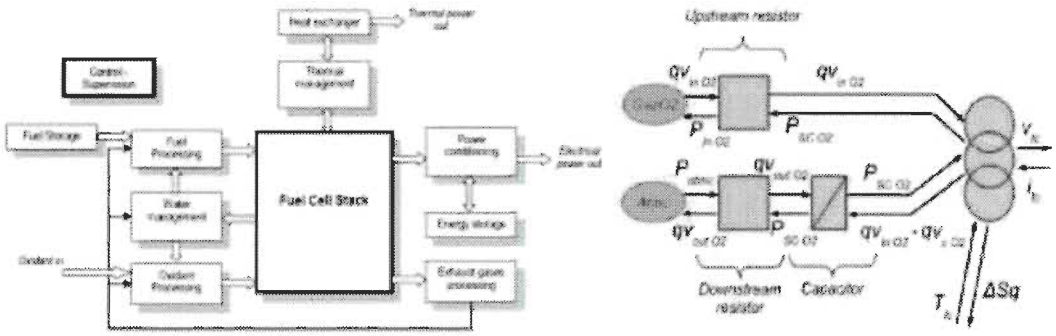

Figure 6-1. Original Nemo EV architecture and modified Nemo HEV architecture[41]

Le système de pile à combustible est un convertisseur d'énergie multi-physique qui implique l'électricité, la thermodynamique, la fluidique et l'électrochimie. Cette méthode se concentre sur la gestion de l'humidité et de l'influence de la direction d'alimentation en air comme la sortie de l'empilement de piles à combustible. En outre, en utilisant une boucle de commande en temps réel pour améliorer la gestion de l'énergie d'alimentation en air, un premier indicateur de la qualité de la gestion de l'eau a été présenté.

Grâce au procédé d'addition dans le compresseur d'air, un résultat significatif de la première analyse pour la gestion de l'énergie est fournie. Les travaux futurs peuvent être commencés par la conception d'une stratégie de contrôle d'alimentation d'air efficace qui devrait être facilitée par la logique floue.

6.1.1.2 Gestion de l'énergie de la batterie

Lors de son stationnement, la puissance de charge est fournie par le réseau. La PEMFC et générateur de moteur à combustion interne seront lancés pendant la conduite.

Comme le montre la figure, PEMFC est ajouté dans le circuit d'exploitation en tant que ressource de puissance. Dans le même temps, le générateur de moteur à combustion est également démarré dans une autre branche. Il agit comme force alternative lorsque le combustible (hydrogène) = 0. Le courant alternatif est fourni par le générateur de ICE. Par conséquent, la batterie plomb-acide sera chargée par le courant continu tandis que le convertisseur continu-alternatif est situé entre le générateur et la batterie. Le courant continu sera contrôlé par le contrôleur principal. Le schéma de principe est présenté en tant que :

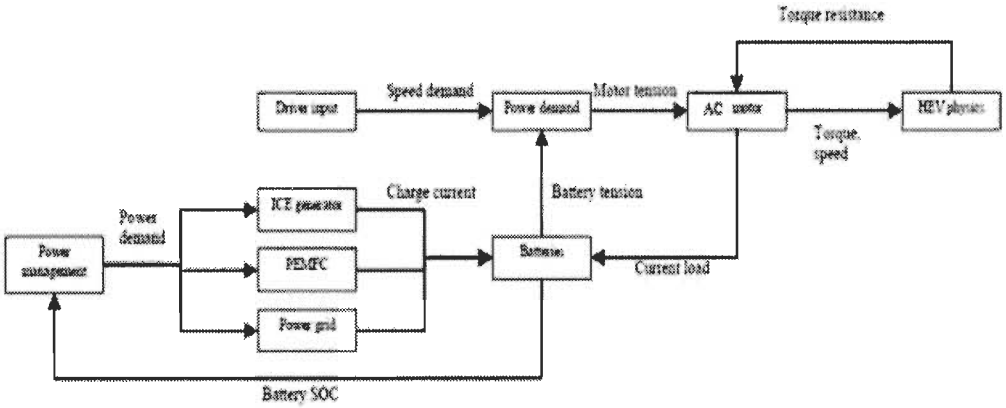

Figure 6-2. Schéma du système de commande de puissance dans le Nemo [41]

Les deux systèmes de charge peuvent travailler de façon autonome. Par conséquent, l'optimisation sera basée sur la branche de circuit de charge PEMFC et l'organisation est représentée comme figure suivante :

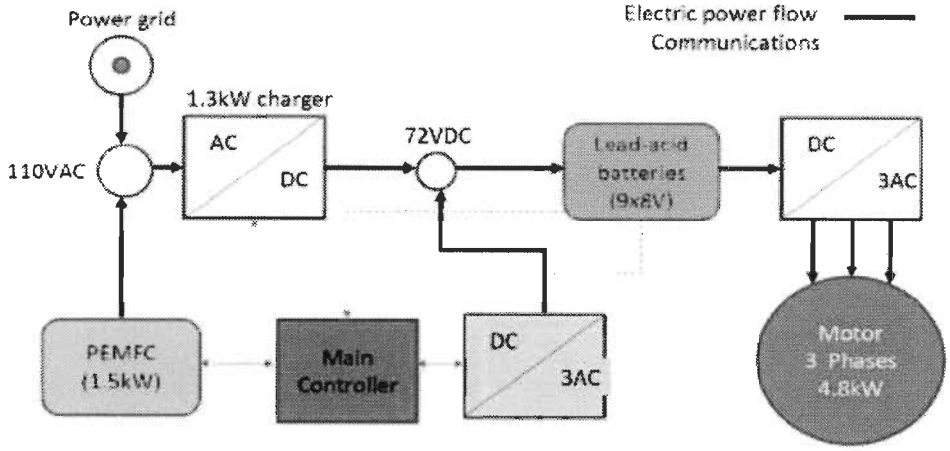

Figure 6-3. Le circuit de charge fourni par PEMFC[41]

6.1.1.3 Expectations d'optimisation - Gestion d'énergie du système de charge

Un autre facteur qui ne peut être ignoré est la consommation d'énergie du circuit de charge. En d'autres termes, la forme de charge et l'efficacité de charge sont des facteurs importants parce que la batterie est purement de la conversion de l'énergie chimique en énergie électrique (ajout à la consommation thermique). Dans le même temps, la durée de vie de la batterie est également affectée de manière significative par les procédés de charge. Par conséquent, la gestion de l'énergie du circuit de charge-décharge va directement affecter l'économie. Il existe des méthodes efficaces pour atteindre l'objectif, comme charge lente et la charge de tension constante.

L'optimisation est mise en œuvre par deux méthodes: la charge d'impulsion et le contrôle des DOD. En utilisant la méthode de l'impulsion de charge, le processus de charge est raccourci ce qui peut réduire le coût de l'hydrogène. En contrôlant la DOD, la vie de la batterie peut être augmentée dans le cas d'une consommation d'hydrogène raisonnable.

6.2 Modélisation de Nemo

La Figure 6-4. **Modèle de système de la NEMO** montre le modèle global du Nemo. Le PEMFC agit en tant que générateur pour charger la batterie. Lorsque l'état de charge

(SOC) est inférieure à la valeur de profondeur de décharge, le générateur se met en marche pour charger la batterie de soutenir la puissance d'entraînement du moteur 3-phrase à travers le convertisseur DC/ AC.

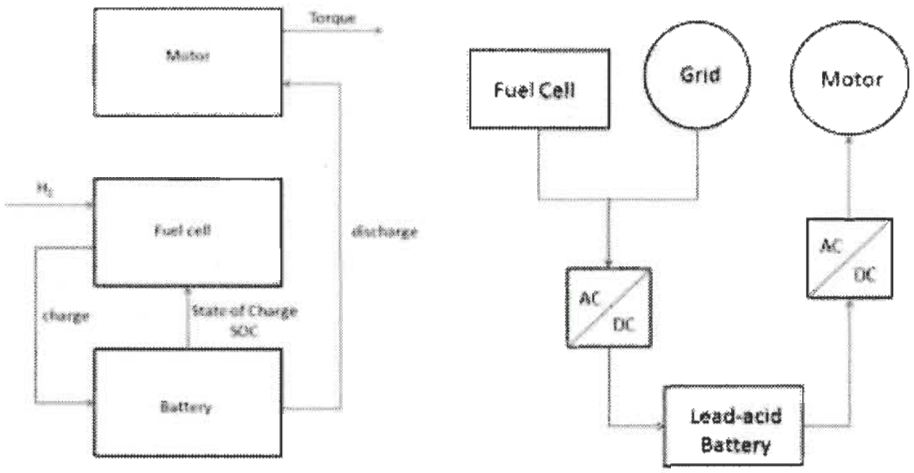

Figure 6-4. Modèle de système de la NEMO

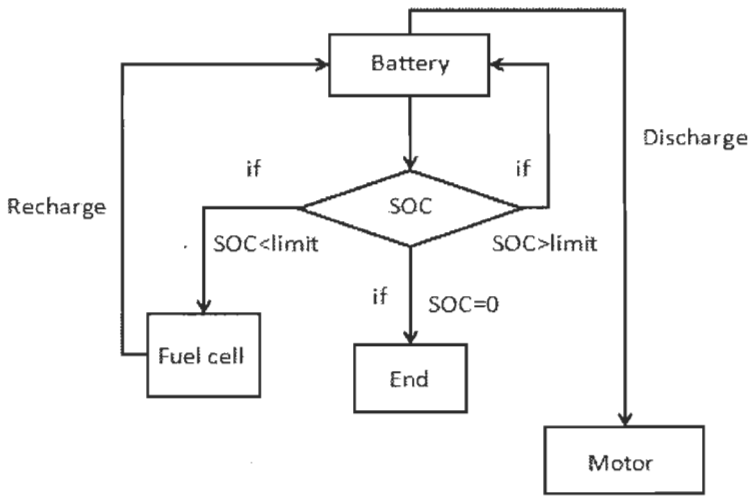

Figure 6-5. Ordinogramme du principe de fonctionnement de Nemo

Si le SOC est plus élevé que la limite fixée, le moteur sera soutenu par batterie uniquement. Alors que le SOC est inférieur à la limite fixée, la pile à combustible sera allumée pour charger la batterie et soutenir la puissance mécanique. Sinon, lorsque l'hydrogène dans la pile à combustible est vide, il n'y aura pas de source pour charger la

batterie et SOC aura tendance à 0%. Ainsi, le modèle total sera terminé et le camion se arrête [27].

6.2.1 Modèle dynamique

Le modèle physique de la situation de conduite peut être exprimé par l'équation suivante:

$$F_{torque} = F_{acc} + F_r + F_{ad} + F_{cr} \tag{6.1}$$

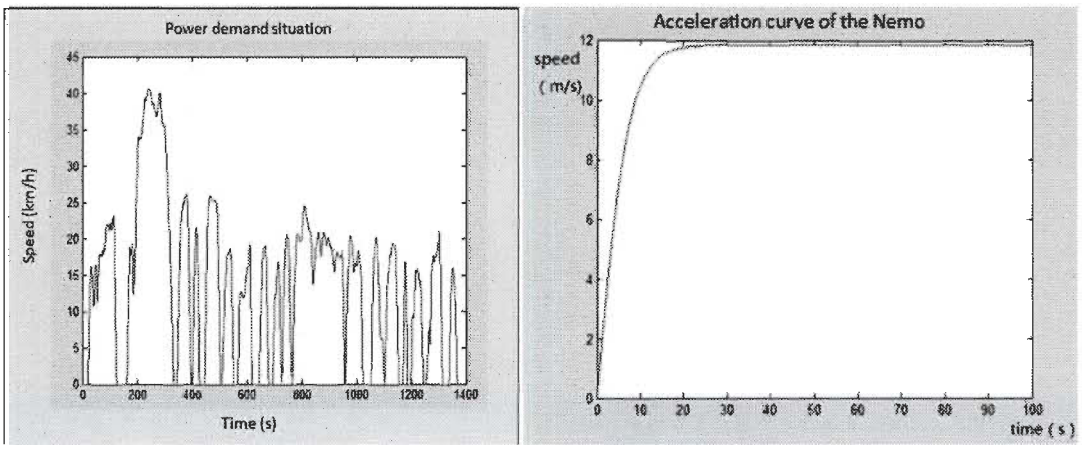

Figure 6-6. Cycle de UDDS (1370 secondes) et l'accélération de Nemo

6.2.2 Modèle du fuel cell

Pour charger la batterie, la sortie de la pile à combustible est la tension. Dans la pile à combustible, la tension n'a pas une valeur constante. Il comporte deux parties principales, la tension de Nernst et de surtension. Dans la pile à combustible, il existe trois formes de surtension, tension d'activation (V_act), tension ohmique (V_ohmic) et de concentration (V_conc).

$$V_{cell} = E_{nernst} + V_{act} + V_{ohmic} + V_{conc} \tag{6.2}$$

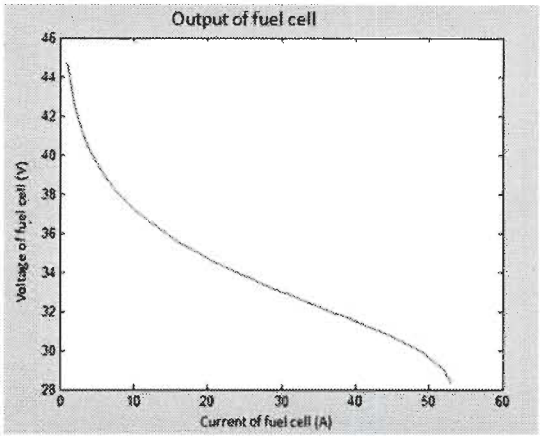

Figure 6-7. Relation de la tension actuelle et des PEMFC

6.2.3 État de la batterie

SOC (état de charge) est la valeur la plus importante lors de la surveillance de la batterie [34]. Dans la Figure 6-8, la batterie (100% SOC) soutenir le fonctionnement du véhicule pendant 10 heures au niveau de puissance de sortie de 2.5kW. Il peut être constaté que la courbe de charge fluctue en dessous de la limite d'ensemble de SOC. Ce phénomène qui illustre le fonctionnement de la pile à combustible est réduit pour ralentir la vitesse de SOC. Charger la batterie à l'état complet n'est pas disponible en raison de la puissance de sortie ne est pas suffisamment élevée. Cependant, l'augmentation du taux de consommation d'hydrogène en "a" est supérieure à "b". Ainsi, la conclusion préliminaire que l'on peut obtenir est de commutation sur la pile à combustible à un niveau inférieur de SOC peut réduire la consommation d'hydrogène. Lors du démarrage de la pile à combustible à un niveau élevé de SOC, plus d'hydrogène sera consommé.

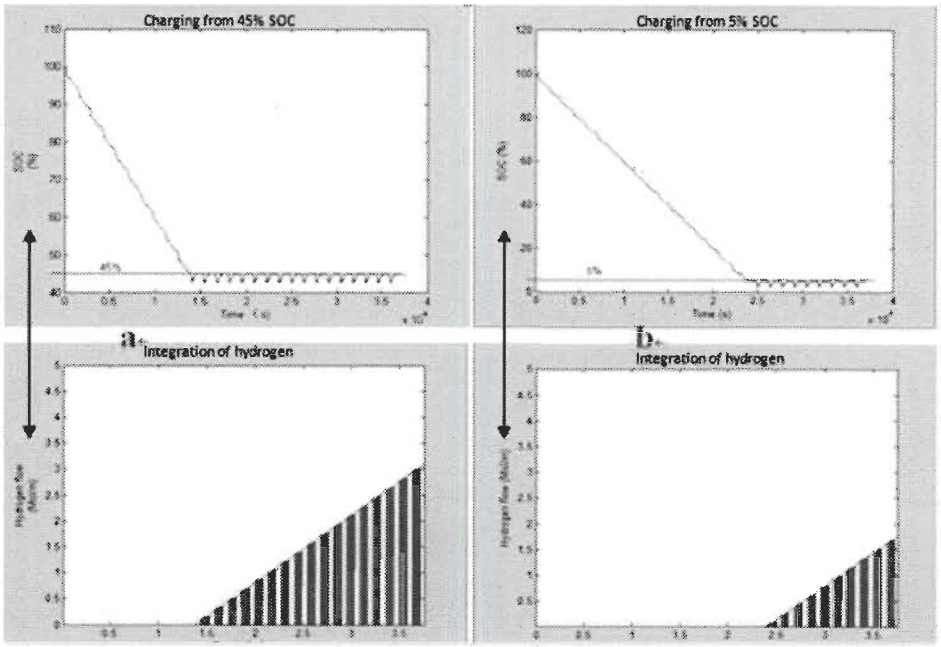

Figure 6-8. Batterie SOC de décharge-charge et la consommation d'hydrogène, un: décharge et l'interrupteur sur la pile à combustible à 5% (SOC); b: Charge de 45% -95% (SOC)

6.2.4 Consommation d'hydrogène

La consommation d'hydrogène est affectée par deux éléments, la série de piles à combustible et le courant de sortie [36]. Ainsi, dans la simulation, les deux paramètres variables qui peuvent être commandés sont sa série et le courant. La consommation d'hydrogène peut être calculée par:

$$Con_{H_2} = \frac{I_{ch} \times N_{fc}}{2F} \times \eta \times t \qquad (6.3)$$

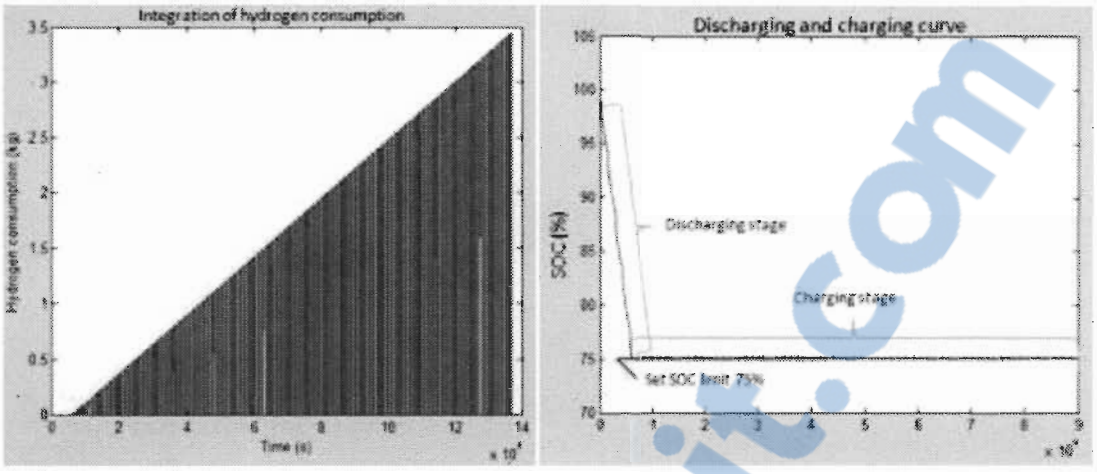

Figure 6-9. a: Intégration de la consommation d'hydrogène; b: SOC de la batterie

6.3 Optimisation de la Nemo

6.3.1 L'optimisation des temps de départ

L'équation suivante est le modèle de l'économie de la consommation d'une opération totalement Nemo.

$$Cost_{Total} = Cost_{hydrogen} + Cost_{battery} + Cost_{fuel\ cell} \tag{6.4}$$

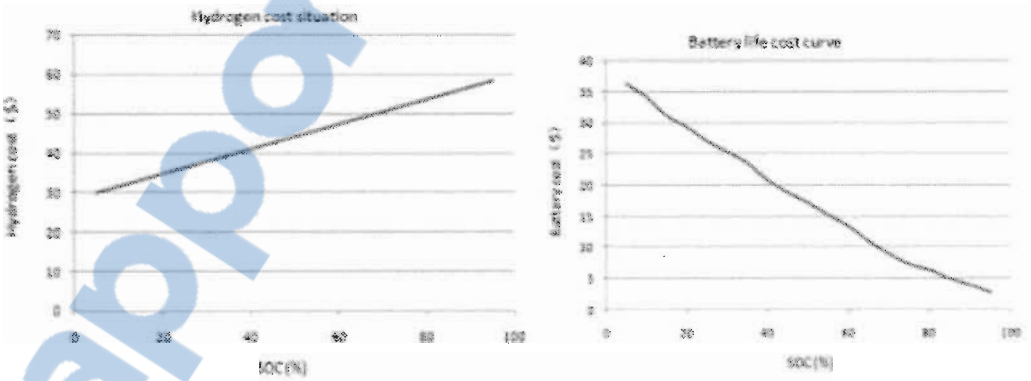

Figure 6-10. Le coût de l'hydrogène et le coût de la batterie

Rapport-Gratuit.com

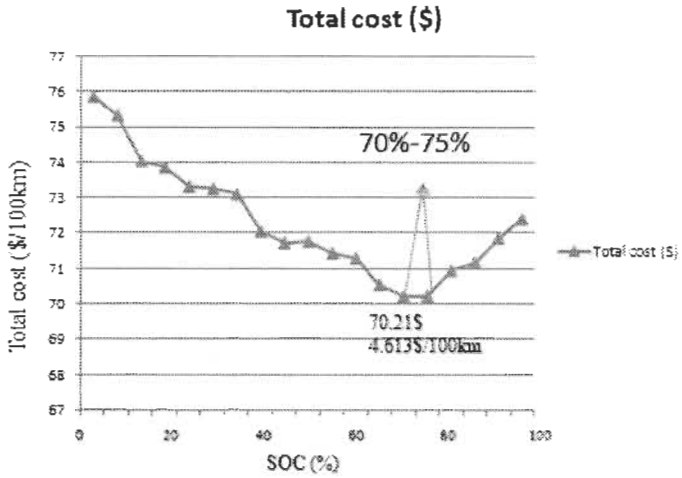

Figure 6-11. La consommation totale de la Nemo

Lorsque la plage de début de la pile à combustible est au SOC 70% -75%, le coût total est le minimum (70.21$). Dans ce cas, le coût par 100 km est d'environ 4.613 $.

6.3.2 Optimisation du circuit

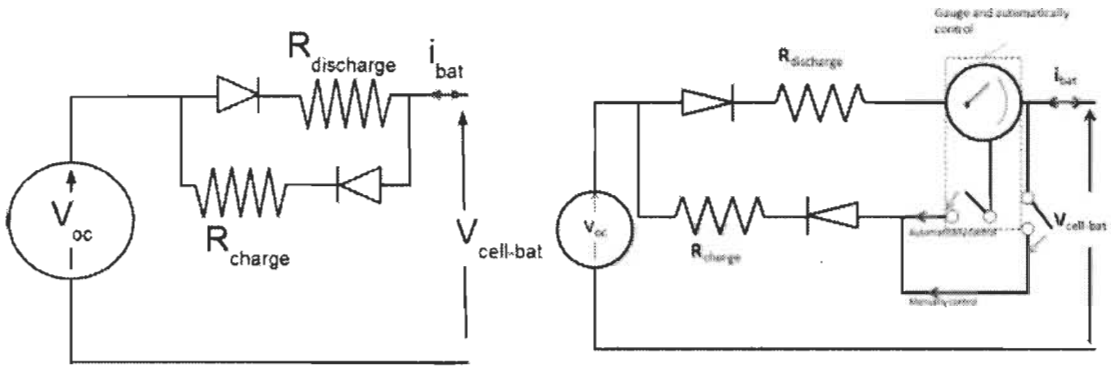

Figure 6-12. Circuit de charge actuel et modidié

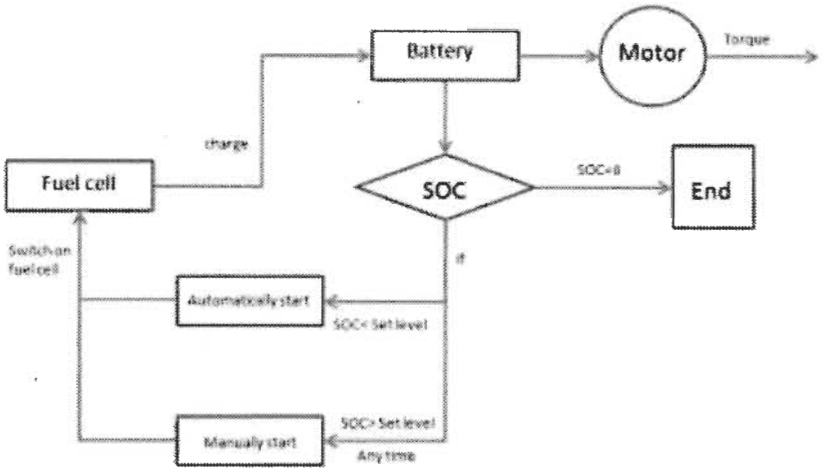

Figure 6-13. Organigramme du circuit de charge automatiquement et manuellement

Deux systèmes de contrôle sont fixés : contrôler automatiquement et contrôler manuellement les deux méthodes existent dans le circuit. Alors que le conducteur oublie ou ne peut pas (laisser le véhicule sans éteindre) pour basculer sur la pile à combustible, le système de contrôle automatique peut commencer la pile à combustible au niveau de la SOC précédemment défini. Alors que le conducteur veut démarrer la pile à combustible (le niveau de SOC est encore plus élevé que le niveau précédent), la pile à combustible peut être mise en marche manuellement aussi. Donc le circuit optimisé réduit les difficultés de fonctionner efficacement.

6.3.3 Poursuite de l'optimisation de la résistance de charge

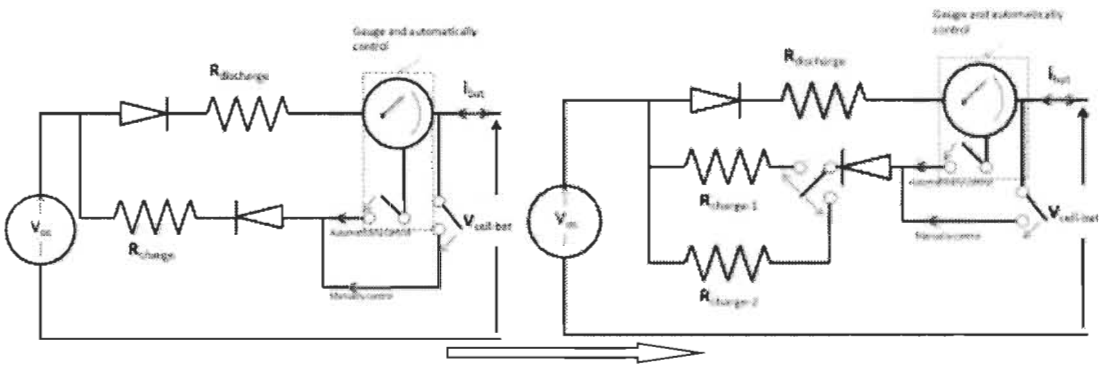

Figure 6-14. Amélioration de la résistance variable

Rapport-gratuit.com
LE NUMERO 1 MONDIAL DU MÉMOIRES

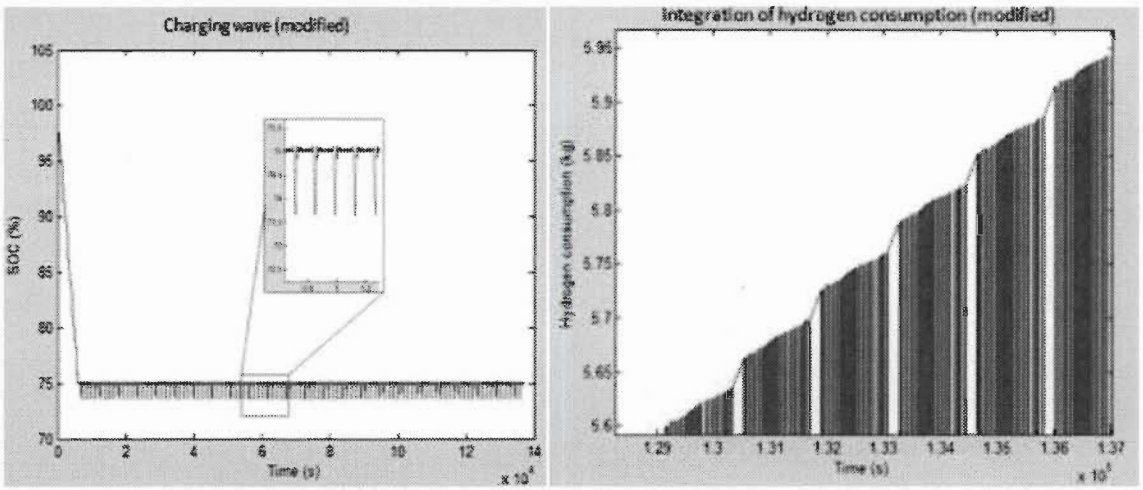

Figure 6-15. Charge situation après modifiée

La volatilité de l'onde de charge diminue de 2.5% à 1.4%. Cela signifie que le DOD réel est de 73.5%. En outre, la consommation d'hydrogène diminue à 5,94 kg (économisez 0.56kg ; ≈9%). L'augmentation du courant est un procédé qui peut réduire le coût de l'opération efficace.

6.3.4 Caculation de l'optimisation des ecnomy

Comme la consommation est la somme du coût de l'hydrogène et le coût de la pile. Par conséquent, le modèle d'optimisation peut être écrit comme:

$$Cost_{Total} = Cost_{hydrogen} + Cost_{battery} + Cost_{fuel\ cell}$$

$$Cost_{Total} = (\frac{I_{ch} \times n_f}{2F} \times \eta) \times (t_1 - t_0) \times A_{cost} + \frac{P_B}{L_B} \times C_{Ch} \times n_B + \frac{Power_f \times Price_f}{Life_f} \times (t_1 - t_0)$$

(6.5)

Le coût de la conversion de l'hydrogène est

$$\Delta_{cost} = (\frac{I_{ch} \times n_f}{2F} \times \eta \times A) \times (t_1 - t_0) + \left(\frac{P_B}{L_B} - \frac{P_B}{L'_B}\right) \times C_{ch} \times n_B$$

(6.6)

Dans l'équation modifiée,

$$L_B = 2500$$

$$L'_B = 2700$$

Table 6-1. L'analyse détaillée des données

SOC (%)	Available charge cycles (Battery)	Hydrogen (original) (kg/100km)	Cost (original) ($/100km)	Hydrogen (optimized) (kg/100km)	Cost (optimized) ($/100km)
5	545	0.246386	4.982278	0.246386	4.765277
10	580	0.25933	4.947959	0.253876	4.700426
15	635	0.272273	4.86341	0.261367	4.589912
20	675	0.285217	4.85173	0.268857	4.545642
25	730	0.29816	4.816248	0.276347	4.479733
30	780	0.311104	4.811736	0.283837	4.441979
35	840	0.324047	4.802328	0.291327	4.399775
40	950	0.336991	4.732727	0.298817	4.30285
45	1050	0.349934	4.712033	0.306307	4.250385
50	1150	0.362878	4.71402	0.313798	4.218539
55	1300	0.375821	4.693217	0.321288	4.165976
60	1475	0.388765	4.684213	0.328778	4.124139
65	1800	0.401708	4.634691	0.336268	*4.045466*
70	2300	0.414652	*4.613009*	0.343758	*4.031438*
75	2700	0.427595	*4.613228*	0.351248	4.156084
80	3100	0.440539	4.660782	0.358739	4.22458
85	4000	0.453482	4.676084	0.366229	4.293075
90	5000	0.466426	4.720762	0.373719	4.36157
95	7000	0.479369	4.756148	0.381209	4.430066

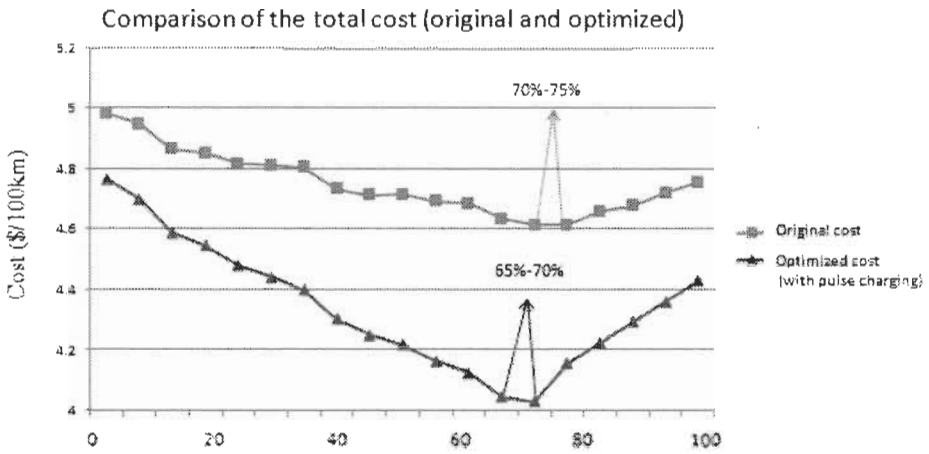

Figure 6-16. Comparaison du coût total

6.4 Conclusion

Le travail consiste en trois parties de l'optimisation, l'optimisation du temps pile à combustible de départ, l'optimisation de circuit de charge et la charge d'impulsion. En optimisant le temps de départ pile à combustible, l'hydrogène et le coût de la batterie seront réduits au minimum et le meilleur temps de fonctionnement de la pile à combustible peuvent être obtenus.

Avec l'optimisation du circuit de charge, le résultat est évidemment représenté. La profondeur de décharge est réduite. La durée de vie de la batterie sera prolongée. Le rendement de charge sera augmenté. Par conséquent, le coût total peut être réduit.

La poursuite de l'optimisation est le procédé de charge d'impulsion et grâce à cette méthode, le temps de charge sera réduit de 10%, ce qui permet de réduire la consommation d'hydrogène. De plus, la surchauffe dans le processus de recharge de la batterie peut être résolue de manière efficace. L'effet du vieillissement peuvent également être réduit. Ces optimisations peuvent étendre les cycles de charge de la batterie.

Table 6-1. **L'analyse détaillée des données** présente la comparaison de la consommation d'hydrogène entre le modèle régulier et optimisé. En réduisant la résistance du circuit de charge, la consommation totale de l'hydrogène peut être enregistré 5% -15%. De SOC 70%

-75% (DOD = 25% -30%) la consommation totale réduite de 14% -16%. La courbe est représentée sur la Figure 6-16.

Figure 6-16 présente la courbe du coût total y compris le coût de l'hydrogène et le coût de la pile. De toute évidence, le modèle modifié réduit le coût final efficacement. En outre, grâce à la réduction de l'amplitude de l'onde de charge, la charge de la batterie sera plus stable. Toutefois, la limite du courant d'entrée est limitée à un maximum 40A. Si une poursuite de l'optimisation est à espérer à atteindre, les problèmes de température et de résistance devraient être résolus d'abord [21].

Appendix B Technical Specifications Manufacturer

Appendix B1 US battery parameters

US 8VGCE XC2, US 8VGC XC2, US 8VGCHC XC2

DATA SHEET Deep Cycle 8 -Volt

Application: Wherever Deep Cycle 8-volt batteries are needed.

Dimensions: 10-1/4 (260)L x 7-1/8 (181)W x 11-1/4 (286)H

Type: Flooded Lead Acid (FLA) non-sealed.

Case material: Polypropylene / Heat Sealed

US 8VGCE XC2, US 8VGC XC2, US 8VGCHC XC2 - SPECIFICATIONS

BCI Group Size	Model	5-Hr Rate	3-Hr Rate	2-Hr Rate	1-Hr Rate	15-Hr Rate	20-Hr Rate	48-Hr Rate	72-Hr Rate	100 Hr Rate	Voltage	Standard Terminal Type	AMP HOURS (20 HR. RATE)	MINUTES @ 25 AMPS	MINUTES @ 56 AMPS	MINUTES @ 75 AMPS	Length	Width	Height	Wet Weight Lbs (kg)
GC8	US 8VGCE XC2	75	84	87	100	106	121	128	132	136	8	UTL	131	60	20	222	10-1/4 (260)	7-1/8 (181)	11-1/4 (286)	56 (25.7)
GC8	US 8VGC XC2	105	118	138	142	163	172	180	186	189	8	UTL	170	90	139	337				64 (29.0)
GC8	US 8VGCHC XC2	150	164	147	192	164	183	194	199	203	8	UTL	185	95	136	365				67 (30.4)

TERMINAL OPTIONS:

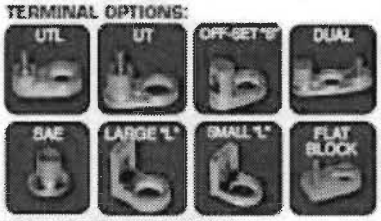

VENT CAP OPTIONS:

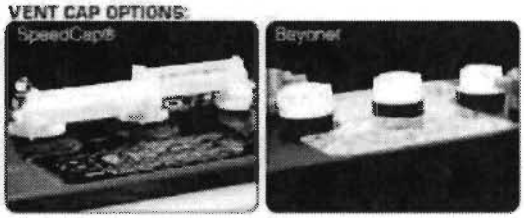

CHARGING INSTRUCTIONS:

Following is the charging recommendation and charging profile using 2 stage chargers for US Battery deep cycle products.
*Equalization and float charge modes are not considered to be one of the stages in a charging profile.

1. **Bulk Charge** — Constant current (8–10% of C/20 Ah in amps to 2.45+/-0.05 volts per cell (e.g. 7.35 volts +/-0.15 volts per 6 volt battery)
2. **Absorption Charge** — Constant voltage (2.45+/-0.05 vpc) to 3% of C/20 Ah in amps then hold for 2-3 hours and terminate charge. Charge termination can be by maximum time (2-4 hr) or dV/dt (4 mv/cell per hour)

- **(Optional Float Charge)** — Constant voltage 2.17 vpc (6.51 volts per 6 volt battery) for unlimited time
- **Equalization Charge** — Constant voltage (2.55+/-0.05 vpc) extended for 1-3 hours after normal charge cycle (repeat every 30 days)

Notes: Charge time from full discharge is 9-12 hours.
Absorption charge time is determined by the battery but will usually be ~3 hours at 2.45 volts per cell.
Float time is unlimited at 2.17 volts per cell.
Specific gravity at full charge is 1.270 minimum

Battery temperature adjustment: reduce the voltage by 0.028 Volts per cell for every 10°F above 80°F, increase by the same amount for temperatures below 80°F.

Deep cycle batteries need to be equalized periodically. Equalizing is an extended, low current charge performed after the normal charge cycle. This extra charge helps keep all cells in balance. Actively used batteries should be equalized once per month.
Manually timed chargers should have the charge time extended approximately 3 hours.
Automatically controlled chargers should be unplugged and reconnected after completing a charge.

For more information or questions, please visit **WWW.USBATTERY.COM**

©2008 U.S. Battery Mfg. Co. All rights reserved

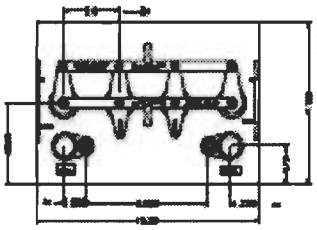

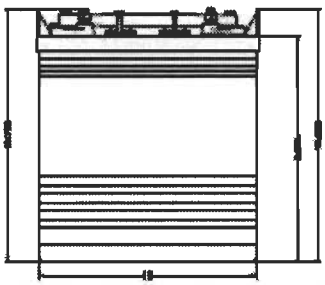

US 8VGCE XC2, US 8VGC XC2, US 8VGCHC XC2

DATA SHEET Deep Cycle 8 Volt

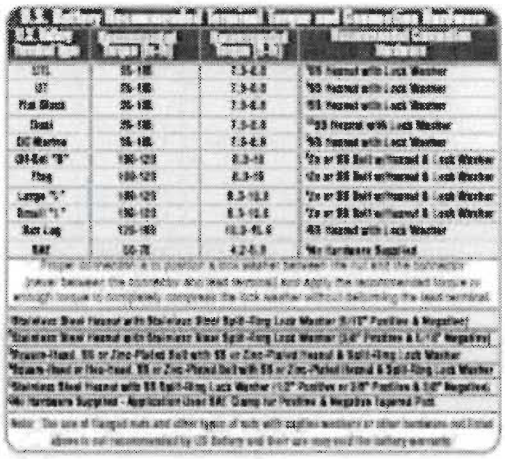

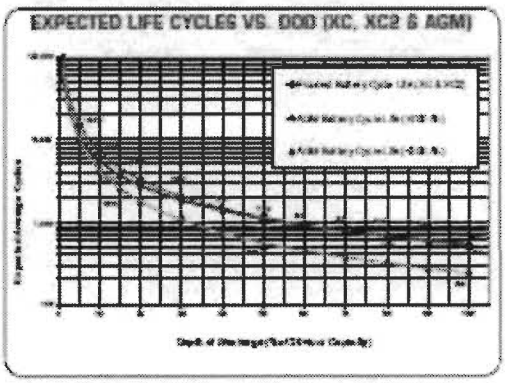

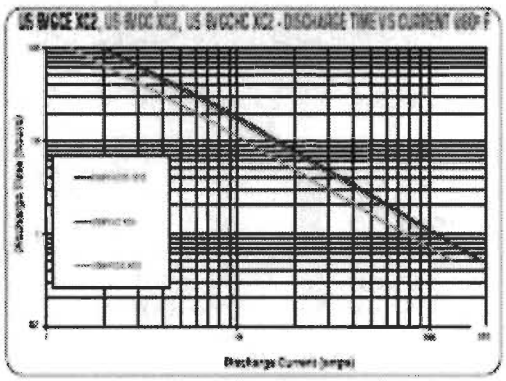

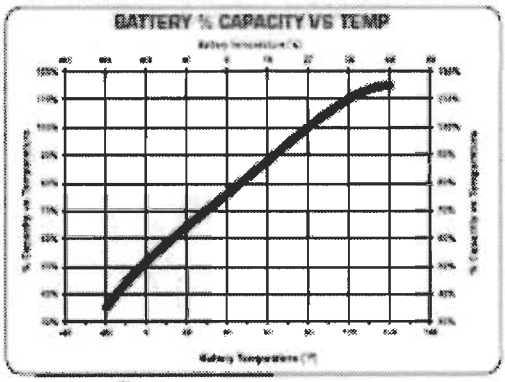

U.S. Battery Operating Temperature Guidelines

For charging, we recommend staying within 0°F to 120°F (-18 to 49°C) to avoid charging frozen batteries at low temperatures or going into thermal runaway at high temperatures.

For discharging, we recommend -50°F to 120°F (-33 to 49°C). Batteries discharged at temperatures below 20°F (-7°C) should be recharged immediately to avoid freezing.

Batteries discharged at temperatures above 120°F (49°C) should be allowed to cool before recharging.

Extreme temperatures can substantially affect battery performance and charging. Cold reduces battery capacity and retards charging. Heat increases water usage and can result in overcharging. Very high temperatures can cause "thermal runaway" which may lead to an explosion or fire. If extreme temperature is an unavoidable part of an application, consult a battery/charger specialist about ways to deal with the problem.

Data references within this publication are nominal and should not be considered or construed as maximum or minimum values for specifications or for final design. Data for the product type and model may vary from what is shown in this publication, and U.S. Battery Mfg. Co. makes no warranties, expressed or implied based on the data within this publication.

©2013 U.S. Battery Mfg. Co. All rights reserved. U.S. Battery is not liable for damages that may occur from any information, omission or conflict from this publication, under any circumstances. U.S. Battery Mfg. Co. reserves the right to make changes or adjustments to this publication at any time, without notice or obligation.

1675 Sampson Avenue
Corona, CA 92879
(800) 695-0945

1895 Tobacco Road
Augusta, GA 30906
(800) 522-0045

717 North Belair Rd
Evans, GA 30809
(888) 811-0045

For more information or questions, please visit **WWW.USBATTERY.COM**

©2013 U.S. Battery Mfg. Co. All rights reserved.

Appendix B2 Parameters of Nemo and the performances

URBAN TRUCK

MUST HD2

This electric LSV truck, designed and manufactured in Quebec, has incredible agility thanks to a tight turning radius, yet offers solid dependability and flexibility thanks to its 1000lbs payload.

Technical Specifications

- General Specifications
- Optional Equipment
- Safety
- Dashboard

Contacts and Addresses

Photos

Media Section

Press Release

About Nemo

Nemo and its team have been researching durable solutions to preserve the environment for the upcoming generations. They have gathered competent specialists in the appropriate fields to create a new type of vehicle using a clean and renewable energy source, ELECTRICITY.

The vehicles offered are technologically advanced and fully compliant with environmental legislation. They are the outcome of a team of engineers, designers and suppliers with a common goal, SAFETY AND ENVIRONMENT.

Nemo

General Specifications

Engine
72 V 5,69KW/8HP AC

CURTIS controler
Thermal protection
Overcharge protection
Braking regeneration
Speed limiter

Batteries
12x6V batteries
12V accessories battery
Centralized battery fill-up

Charger
Smart charger
110V inlet
1100W Power
Charging time : 80% 6h*-12h maximum

Heater
1400W

Transmission
Rear-wheel drive

Chassis
Aluminum tub

Body
ABS panels on aluminum structure

Doors
Tubular doors

Windshield
Tinted windshield

Brakes and suspension
Front and rear disk brakes
4-link solid axles
Coilover springs
Hydraulic shocks

Steering
Rack and pinion
Adjustable steering wheel

Wheels
13in alloy rims
175/70R13 radial tires

Range and speed
Top speed : 40km/h or 25mph (governed)
Range : 115kms or 70mi

Dimensions

Width	1m52	60in
Length	3m48	137in
Heigth	1m90	75in
wheelbase	2m05	80.7in
Turning radius	4m42	174in
Cargo area	2m13x1m52	7'x5'
Weight	896kgs	1980lbs
Payload	453kgs	1000lbs

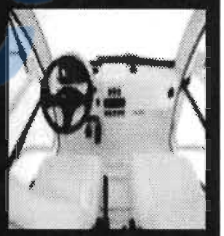

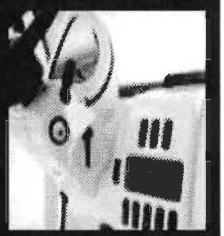
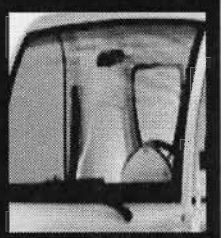

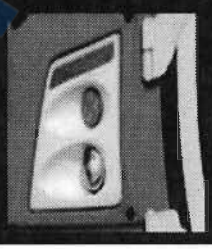


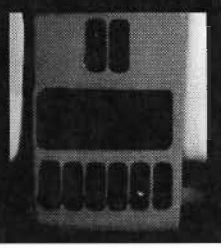

Rapport Gratuit.com

Nemo

Safety

- Cockpit integrated rollcage on reinforcement beam
- Lateral safety beam
- 3 point safety belts
- Battery pack separated from passenger area
- 50/50 weight distribution and very low centre of gravity
- 4 wheels hydraulic disc brakes
- Power cut-off switch
- 3 braking lights (bumper and roof mounted)
- 55W halogen headlights
- Roof mounted strobe light
- Multiple intensity horn (for road or pedestrian applications)
- Tinted laminated windshield with wipers, washers and electric embedded defroster
- Heater and air defroster
- Adjustable steering wheel
- Secure anti-theft ignition key
- Data acquisition ECU (black box)
- Reverse lights and alarm

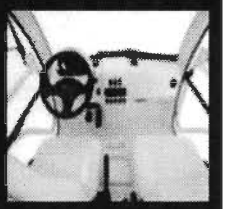

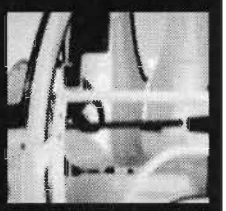

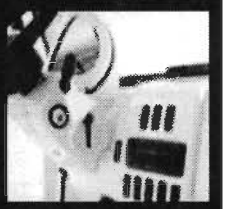

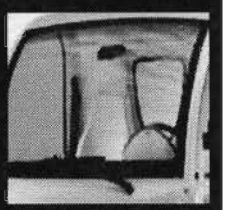

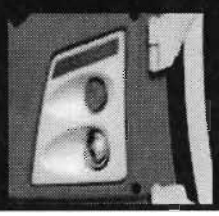

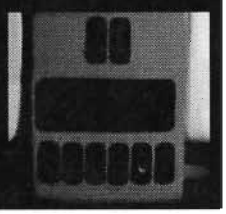

Dashboard

Dials and indicators

- Energy demand
- Speed
- Battery charge status
- Battery temperature
- Battery check
- Engine check
- Speed limiter
- Handbrake
- LCD display
- Vehicle status sound feedback

Switches

- Ventilation
- Heater
- Horn mode
- Speed limiter
- Forward/Reverse selector
- Stalks
- Interior lighting

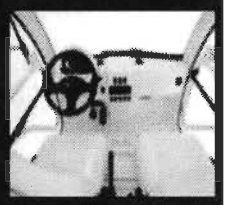
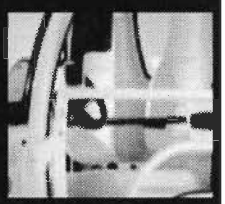
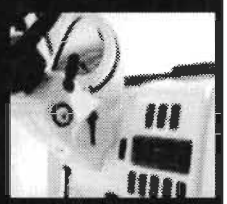


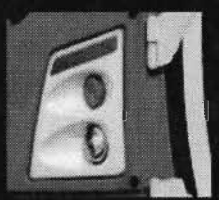

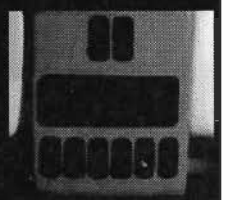

Rapport-gratuit.com
LE NUMERO 1 MONDIAL DU MÉMOIRES

Options (standart flatbed cargo area)

- Fold-down sides (2m10x1m50x28cm)
- Enclosed (poles and tarp)
- Full height box with lateral grill
- Folding tailgate
- Electrics pack
  - Roof strobe
  - Accessory 12V plug
  - Dome light
  - AM/FM/CD Radio
- Auxiliary 50W headlights
- Central console and cupholders
- Lateral trunks
- Bumpers
- Quick charging system (*6h charging time)
- Cargo light
- Lithium batteries
- Flashing arrow

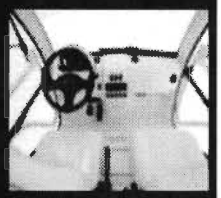

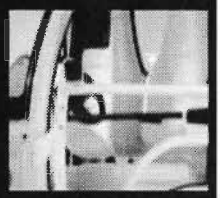

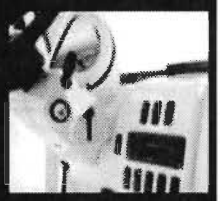

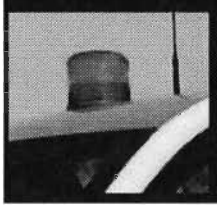

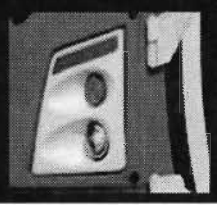

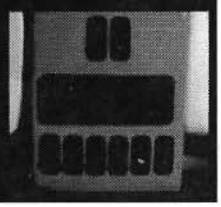

Battery charger - PFC2000+

PFC2000+

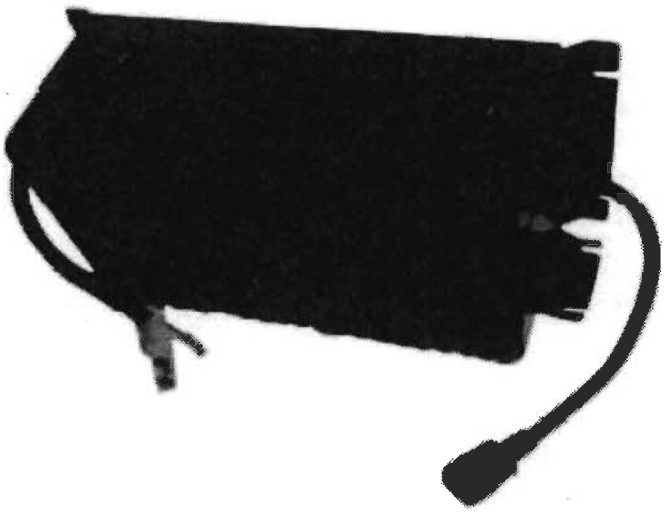

Description

- Advanced high frequency switching design with 92% typical efficiency
- Fully sealed enclosure providing improved reliability in demanding environments
- > 0.98 Power Factor minimizes utility surcharges and maximizes use of AC power
- Approved battery charge algorithms for ideal charging (default I1, I2, U, I3a)
- Memory to store 10 unique algorithms, and tools to load new algorithms in the field
- The internal CPU employs advanced charging management algorithm

Technical Features

DC Output

Model	36XX	48XX	60XX	72XX	84XX	96XX
DC Output Voltage - nominal	36V	48V	60V	72V	84V	96V
DC Output Voltage - maximum	51V	68V	85V	102V	119V	136V
DC Output Current - 230vac	40A	30A	25A	21A	18A	15A
DC Output Current - 115vac	35A	28A	25A	19A	17A	14A
Model	**120XX**	**144 XX**	**156XX**	**168XX**	**288XX**	
DC Output Voltage - nominal	120V	144V	156V	168V	288V	
DC Output Voltage - maximum	170V	204V	221V	238V	408V	
DC Output Current - 230vac	13A	11A	10A	9A	5.5A	
DC Output Current - 115vac	12A	10A	9A	8A	5A	
Battery Type	Specific to selected algorithm					
Reverse Polarity	Electronic protection – auto-reset					
Short Circuit	Output closed automatically					

Appendix C Simulation Code in Matlab

Appendix C1Dynamic model of Nemo

```
%%%%%%%%%%%%%%%%%%%%%%Dynamic Model%%%%%%%%%%%%%%%%%%%%%%
clc;
clear all;
load UDDS.mat
UDDS=UDDS.*(40/90)./3.6; %Urban Dynamometer Driving Schedule of Nemo
h=1;
t=1:137000;                 % total test time =100*UDDS cycles
v = zeros(1,length(t));
v(1)=0;                     %Initial speed
C_rr=0.01;                  %Coefficient of friction
m=864;                      %mass(vehicle + fuel cell)
g=9.81;                     %Gravity
alpha=0;                    %10%=0.1
rou=1.2      ;              %20C
C_x=0.42;                   %Air resistance
A=4;
%accel(t)=(UDDS(t)-UDDS(t-1))/dt:
dt=1;
rad=0.28829;
F_T=zeros(length(t),1);

For i=2:length(t)
accel(i)=(UDDS(i)-UDDS(i-1))/dt;

F_T(i)=m*accel(i)+0.5*rou*C_x*A*(UDDS(i))^2+m*g*sin(alpha)+m*g*C_rr*cos(alph
a);
Pmec(i)=F_T(i)*(UDDS(i)/rad);
```

```
end
%%%%%%%%%%%%%%%%%%%%%%%%%%%%%%%%%%%%%%%%%%%%%%%
```

Appendix C2 Batter and Fuel Cell Model

```
%%%%%%%%%%%%%%%%%%%%%%%%%%%%%%%%%%%%%%%%%%%%%%%%
V_Fc=72;%Output voltage of fuel cell
I_Fc=Pmec./V_Fc;
Ch=0;
Ca=180;%Ah/3600=A.s
P_fc=1:100:137001;%100 UDDS cycles (time step=100s)
hhv=14190;
SOC_limit=75; %SOC level to start fuel cell
%%%%%%%%%%%%%%%%%%%%%%%%%%%%
ifSOC_limit>75
I_Re=0;
P_fc=0;
else%Condition of execution command
I_Re=20;
P_fc=2500;
end
%%%%%%%%%%%%%%%%%%%%%%%%%%%%
Rech_current=P_fc/72;
c=0;
ikg_H2=0;
tt=0;
Id=0;
dt=1;
for day=1:2%operation loop
for c=1:3
fori=1:dt:length(t)
tt=tt+1;
Ch=((I_Fc(i)-I_Re)*dt)/3600+Ch;
Charge(tt)=Ch;
```

```
%%%%%%%%%%%%%%%%%%%%%%%%%%%%%%
if Charge(tt)>=Ca
Charge(tt)=Ca;
end
SOC(tt)=100-(Charge(tt)/Ca)*100;
ifI_Fc(i)<0%until capacity=0%discharging circuit
                    Id=(0-I_Re)+Id;
else
                    Id=(I_Fc(i)-I_Re)+Id;
end
%%%%%%%%%%%%%%%%%%%%%%%%%%%%%%
Ideg(tt)=Id;
Deg(tt)=(Ideg(tt)*dt/3600)/150000;% Batter aging model
%%%%%%%%%%%%%%
if SOC(tt)<SOC_limit
I_Re=Rech_current;%Charging circuit
%for t=i:length(t)
%fuel cell start charging
Ch=((I_Fc(i)-I_Re)*dt)/3600+Ch;%until hydrogen =0
Charge(tt)=Ch;
if Charge(tt)>=Ca;
Charge(tt)=Ca;
end
%%%%%%%%%%%%%%%%%%%%%%%%%%%%%%
SOC(tt)=100-(Charge(tt)/Ca)*100;
iP_fc=P_fc*(1/hhv)/1000;
                    ikg_H2=iP_fc*dt+ikg_H2;
Con_H2(i)=(((I_Re*48)/96485.3383)*0.8)*2*137000/1000;%SOC and H2 monitor
                    kg_H2(tt)=ikg_H2;
%%%%%%%%%%%%%%%%%%%%%%%%%%%%%%
if SOC(tt)>=95
```

```
SOC(tt)=95;
end
else
I_Re=0;
end
end
end
end
```

Rapport-Gratuit.com